LSU Master's Theses   Graduate School

2007

The role of toll-like receptor 7 in the neuropathogenesis of retrovirus infection in neonates

Stephanie Diane Lewis
Louisiana State University and Agricultural and Mechanical College

Follow this and additional works at: https://digitalcommons.lsu.edu/gradschool_theses

 Part of the Veterinary Pathology and Pathobiology Commons

THE ROLE OF TOLL-LIKE RECEPTOR 7 IN THE NEUROPATHOGENESIS OF
RETROVIRUS INFECTION IN NEONATES

A Thesis

Submitted to the Graduate Faculty of the
Louisiana State University and
Agriculture and Mechanical College
in partial fulfillment of the
requirements for the degree of
Master of Science

in

The Interdepartmental Program in
Veterinary Medical Sciences
through the
The Department of Pathobiological Science

by
Stephanie D. Lewis
B.S., University of Minnesota, 1999
D.V.M., University of Missouri, 2003
May 2007

Finally, I would like to take this opportunity to thank my Master's Thesis committee, Drs. David Baker, Stephania Cormier, and Karin Peterson, for their guidance and patience while encouraging me to excel as a scientist. Karin Peterson, however, deserves a special thank you, for her cooperation, time, and patience in teaching me not only the appropriate laboratory skills required to complete this research project, but also the love for the human element of the scientific process, with its shortcomings, versatility, and creativeness. Karin's knowledge and enthusiasm have inspired me, and her faith and encouragement have been without bound. I am very grateful to her and all of those who supported me.

Table of Contents

Abstract

Viral infections of the central nervous system (CNS) in infants are rare; however, they are associated with high morbidity and mortality rates. These virus infections often induce strong innate immune responses in the brain including: the production of cytokines and chemokines, the activation of astrocytes and microglia and the recruitment of macrophages. Innate immune responses are often initiated by toll-like receptors (TLR). Several studies have demonstrated that toll-like receptor 7 (TLR7) can be stimulated by single-stranded RNA from multiple viruses. In the current study, we examined the mechanism by which TLR7 contributes to neuroinflammation in the neonatal brain using a mouse model of polytropic retrovirus infection. We found that TLR7 deficiency had no effect on neurologic disease, viral replication, or induction of interferon beta mRNA. However, TLR7 deficiency significantly altered neuroinflammatory responses including proinflammatory cytokine production, astrocyte activation, and microglial/macrophage activation. To our knowledge, this is the first demonstration of the necessity of TLR7 for innate immune responses to retrovirus infection *in vivo*. Additionally, this indicates that the immune response to retrovirus in the CNS may not be essential for disease pathogenesis in neonates.

Chapter 1: Introduction

Fr98 infection of neonates induces the innate immune response (1, 2). Activation of microglial cells and astrocytes is observed as well as the production of proinflammatory cytokines and chemokines as detected by both mRNA and protein expression (3-12). Induction of the innate immune response may play a role in either suppression of viral replication or detrimental pathology induced by the viral infection (13-16). Since innate immune responses are often initiated by stimulation of toll-like receptors (17), their study is warranted to discover opportunities to intervene and treat neuropathogenic viral infections in newborns. Toll-like receptor 7 (TLR7), which is activated by single-stranded RNA from numerous viral families (18-22), is expressed on brain capillary endothelial and microglial cells in neonates (23). The role of TLR7 in retroviral infection and the induction of the innate immune response in the neonatal brain are unknown. We hypothesize that TLR7 stimulation by virus infection initiates neuroinflammatory pathways in the developing brain.

To determine the role of TLR7 in the virus-mediated host neuroinflammatory response, we characterized the neuroinflammatory response to Fr98 retrovirus infection in wildtype, heterozygous, and TLR7-deficient mice prior to clinical disease as well as in animals exhibiting clinical signs of disease. Quantitative reverse transcriptase real time polymerase chain reaction technology and multiplex analysis of cytokine and chemokine proteins were utilized to calculate differences in gene expression levels between Fr98-infected and mock-infected wild type and TLR7-deficient animals to determine which neuroinflammatory pathways are dependent on TLR7 stimulation.

Additionally, since the role of TLR7 in retroviral neuropathogenesis is unknown, we infected wildtype, heterozygous, and TLR7-deficient mice with Fr98 retrovirus and followed them for clinical signs of disease. Mice were scored as having neurologic disease when signs of severe ataxia and/or seizures were apparent. Survival curve analysis of disease onset was calculated to determine if TLR7 deficiency altered Fr98-induced neuropathogenesis.

Chapter 2: Review of Literature

2.1: Innate Immune Response in the Brain

The brain is considered an immunologically privileged site due to the lack of lymphatics and the presence of the blood brain barrier (BBB) that restricts immune cell entry into the central nervous system (CNS). However, the immune privilege of the CNS is incomplete. Inflammation can still occur in the CNS, by either a response to exogenous antigens or self-antigens (autoimmunity) (24). Additionally, the innate immune response in the brain may differ between adult and neonatal animals. While adult and neonatal animals both possess tight junctions present at the blood-brain and blood-cerebrospinal fluid (CSF) barriers, neonates also have additional types of junctions (plate, strap, wafer) at the CSF-brain barriers that are not present in adults. The developing brain is also more permeable to small insoluble lipid molecules and has specific transfer mechanisms for certain proteins into CSF (25).

The innate immune system in the brain is composed of phagocytic cells (monocytes/macrophages and polymorphonuclear phagocytes), natural killer cells, interferons, and soluble factors (24). In addition, parenchymal macrophages, microglial cells, and astrocytes also play a role in innate immunity. Key players in the innate immune response in the CNS are microglia/macrophages. The CNS endogenous microglia share many properties with macrophages since they develop from the same hematopoietic line (26-28). When activated, both systemic macrophages and microglial cells are able to phagocytize pathogens, cells, and cellular debris (28-31). There are two types of microglial cells in the CNS, parenchymal microglia and perivascular microglia.

The parenchymal microglial cells are not routinely repopulated by "fresh" monocytes, but perivascular microglial cells are (32). When parenchymal microglial cells are not activated, they play a role in signaling and support to neurons and astrocytes.

Astrocytes, which were once considered just "scaffolding" to support neurons, have recently been shown to actively engage in critical events in the brain such as regulation of the BBB permeability and entry of inflammatory cells (33), antigen presentation (34, 35), and uptake of neurotransmitters (36). Astrocytes possess endfoot processes which are in close physical proximity to the endothelial cells of the blood brain barrier. This location places astrocytes in an ideal position to modulate the transendothelial migration of blood cells into the brain parenchyma (37). Experimentation with angiotensin-deficient mice demonstrated that restoration of the blood brain barrier after injury was strictly dependent upon intact astrocyte function. It has also been shown that monocyte-chemoattractant protein-1 produced by astrocytes direct the migration of monocytes and lymphocytes across the endothelium of an *in vitro* blood brain barrier model (38). Additionally, astrocytes respond to brain injury via reactive gliosis, which is a proliferation of astrocytes in the damaged CNS. Brain lesions of varying etiologies such as infection (i.e. HIV), autoimmunity (MS), degenerative disorders (AD), ischemic or tumor damage are infiltrated by hypertrophic astrocytes expressing elevated levels of glial fibrillary acidic protein (GFAP) (39). Reactive astrocytes also display an increased expression of adhesion molecules compared to resting astrocytes, as well as an increase in the production of cytokines, chemokines, growth factors, and neuropeptides, confirming the involvement of these cells in immune responses (40).

2.2: Toll-like Receptors (TLRs)

The ability of the immune system to detect and recognize pathogens is critical for mounting the appropriate immune response to adequately combat invading organisms. In mammals, host defense against pathogens is dependent on two types of immunity, innate immunity and acquired immunity (41). Pathogen detection by the innate immune system occurs via pattern recognition receptors (PRRs), a class of immune-sensor molecules that recognize microbes or microbial components. This recognition results in the initiation of anti-pathogen gene expression that promotes the adaptive immune response (42). Toll-like receptors are a class of PRRs that detect an array of pathogens (43). The TLR family currently consists of 11 members (TLR1-TLR11) identified in humans, and 12 TLRs identified in mice. TLRs are expressed primarily on cells which are likely to be the first to encounter antigens (44-50), with dendritic cells, macrophages, and neutrophils expressing the highest amount of receptors (51, 52). However, it appears that the majority of the cells in the body express at least a subset of TLRs (53).

All of the TLRs are structurally similar (50). They are all type 1 transmembrane proteins with a single domain that spans the membrane. While the majority of TLRs are expressed on the surface of the cell, some are retained intracellularly, which allows for optimal positioning to interact with certain pathogens invading the host (Fig. 1). For example, TLRs 3, 7, 8 and 9 tend to localize on endocytic compartments (53). The cytoplasmic region of the TLRs consists of a conserved domain (Toll/IL-1R) which contains the cytosolic adaptor protein, myeloid differentiation factor 88 (MyD88), and is responsible for intracellular signaling initiation. Signaling pathways can be MyD88-dependent or MyD88-independent, with TLR3 and TLR4 signaling being the latter (54,

55). MyD88 activation results in NF-κB and mitogen activated protein kinase (MAPK)

activation which results in the secretion of cytokines (55).
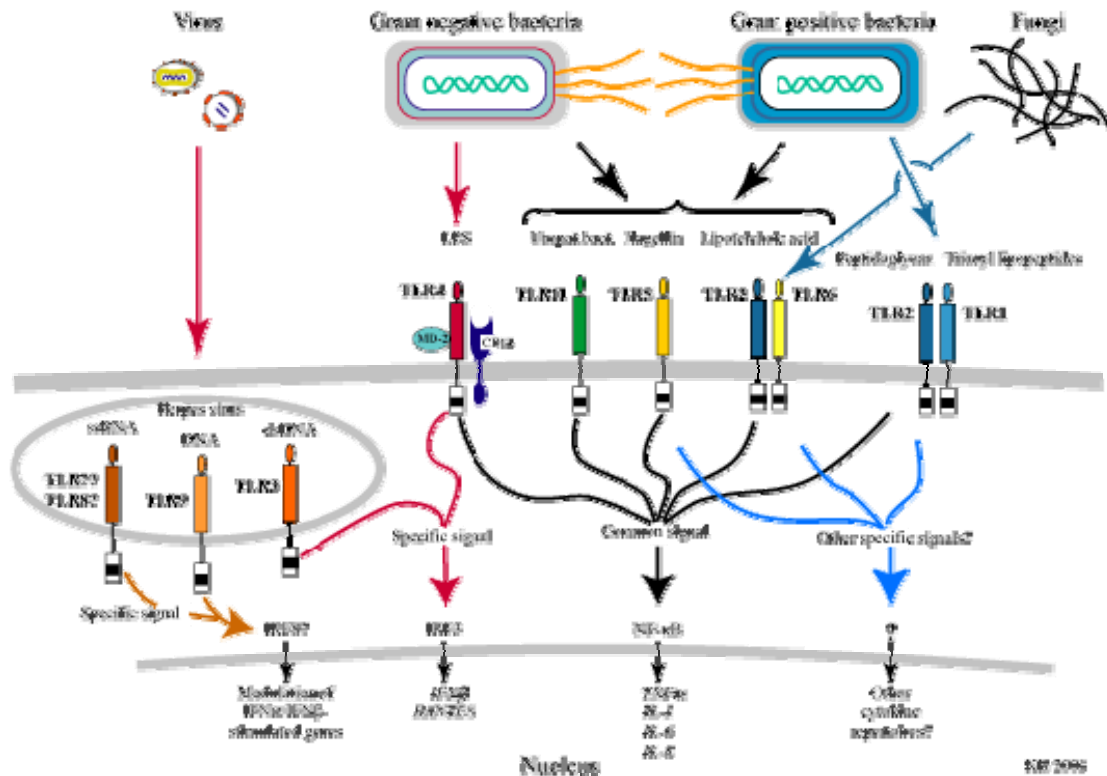
Figure 1. Toll-like receptors and their ligands, cellular locations, and secondary signaling
pathways (53).

The outer domains of TLRs are composed of varying length leucine-rich repeats,

which allows each TLR to recognize specific components of different pathogens,

providing ligand-specific activation. The pathogen-specific motifs on invading

organisms that allow for specific TLR recognition are known as pathogen-associated

molecular patterns (PAMPs) (53). Examples of PAMPs recognized by TLRs include:

lipopolyscaahride (TRL4) (56-58), flagellin (TRL5) (59), peptidoglycan and lipoproteins

(TRL2) (60-63), and deoxycytidylate phosphate deoxyguanylate (CpG) DNA (TLR9)

(64, 65) (Fig. 1). Additionally, some TLRs work together in concert which results in even greater ligand recognition specificity.

Pathogen activation of TLRs results in complex changes in the cellular microenvironment that leads to the activation of the immune system. With regard to viral infections, the purpose of TLR activation and immune system stimulation is to effectively limit the replication and spread of the viral infection. When a TLR is engaged, TLR signaling occurs which leads to induction of NF-kB, causing the transcription of chemokines, proinflammatory cytokines, and the up-regulation of cell surface molecules that are involved in the initiation of the adaptive immune response (66). Experiments in mice and cultured human cells have shown that TLRs also influence adaptive immunity by activating dendritic cells (DCs), which present antigen to T cells and release factors that stimulate T cell differentiation and expansion (67). In addition to the stimulation of humoral immunity by DCs, it has been shown in mice that direct activation of TLRs on B cells is necessary for robust production of some classes of antigen-specific antibodies (68). Therefore, TLRs play an influential role in the activation and stimulation of both the innate and adaptive immune responses.

Recognition of viruses by TLRs also results in stimulation of the antiviral effector type I interferon (IFN) cytokine system consisting of IFNα, IFNβ, IFNω, and IFNτ (69). The production of type I IFNs plays a critical role in antiviral activity because the cytokines both establish an anti-viral microenviroment and bridge the innate and adaptive immune responses (70). Human DCs have been shown to be activated via TLRs to make IFNα in response to multiple enveloped viruses, including influenza virus and HIV. IFNα stimulates multiple protective pathways, such as enhancing the cytotoxic effect of

7

natural killer cells and macrophages as well as stimulation T cell production or maintaining activated T cells (71-74). IFNα has also been shown to induce Th1 activity in human CD4+ T cells (75). Additionally, IFNα also stimulates intracellular RNAse activity, which inhibits viral replication and can lead to viral clearance.

2.3: TLRs and Viral Infection

There are currently four classes of viral PAMPs that are recognized by TLRs which include: double stranded RNA (dsRNA), single stranded RNA (ssRNA), CpG DNA, and envelope glycoproteins (53). It is currently thought that viral ligands come into contact with TLRs in antigen presenting cells (APC) through receptor-mediated uptake of virus or viral fusion with endosomal membranes (76) (Fig. 2). For viruses that either do not infect or cannot replicate in APCs, CD8+ T cells can be activated by cross-priming from DCs that engulf and then present antigen from apoptotic cells infected with virus (67). An example of such an activation system is TLR3. TLR3 recognizes dsRNA and its synthetic analogue, polyinosine-polycytidylic acid (polyI:C) (77). Since dsRNA is a replication intermediate of RNA viruses, it is thought that TLR3 is activated when virus-infected cells are lysed, releasing the dsRNA into the microcellular environment. TLR9 is activated by CpG DNA (64, 65), which is thought to be exposed when virus particles are taken into cells and degraded by endosomal acidification (Fig. 2). TLR9 activation and resultant IFN response occurs only in a MyD88-dependent fashion (78-80). The viral PAMP for TLR7 and TLR8 is ssRNA, which requires endosomal acidification and MyD88-dependent IFN production like TLR9 (18, 19). Because of these similarities between TLR7, TLR8, and TLR9, they are thought to have evolved from a common precursor and operate as a subfamily (49, 81). Viral envelope glycoproteins can

8

act as PAMPs to activate TLR2, TLR3, and TLR4. These are unique in that the virus can

be detected at the earliest stage of infection, before viral gene expression or replication

occurs (53).
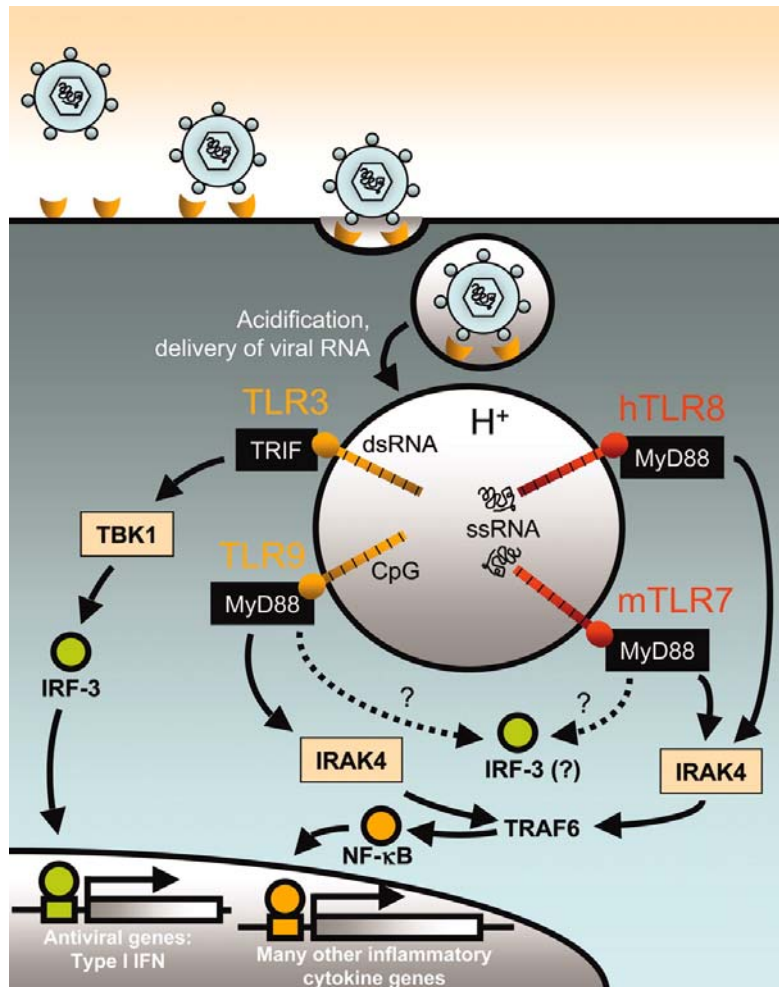
Figure 2. Viral stimulation and signaling pathways of endosomal toll-like receptors (76).

The identification of ssRNA as a ligand for TLR7 is a recent finding. During early

TLR research, the only known ligands of TLR7 and TLR8 were the family of

imidazoquinolines. Imidazoquinolines are low-molecular weight compounds that display

anti-viral and anti-tumor activity and are potent activators of immune cells (82-87). One

imidazoquinoline family member, imiquimod, is currently used as an approved anti-viral treatment in humans with human papillomavirus infections (88). From imiquimod a more potent compound was derived, resiquimod (R-848). Through the use of MyD88-and TLR7-deficient mice, both imidazoquinoline compounds have been shown to stimulate immune cells via TLR7. Imidazoquinoline signaling, cytokine production by macrophages, proliferation of splenocytes, and maturation of dendritic cells were all absent in the MyD88-and TLR7-deficient mice stimulated with imidazoquinolines (89). Additionally, guanosine analogues have also been shown to activate TLR7 and TLR8 (89-92). This discovery resulted in the investigation of ssRNA as a physiologic ligand, since the structure of the guanosine analogues is similar to that of nucleic acids (19). However, TLR7-deficient mice do not respond to imiquimod, R-848, or viral ssRNA, which suggests that murine TLR8 was inactive (19, 89). Recent studies have demonstrated that murine TLR8, along with human TLR8, can be stimulated by the co-administration of TLR7/8 ligands and poly-T oligodeoxynucleotides (pT-ODNs). Administration of the pT-ODN stimulates TLR8, but inhibits TLR7-mediated responses (93-95). To date, genomic RNA from influenza A virus, vesicular stomatitis virus, and synthetic RNA oligonucleotide from human immunodefiency virus type-1 (HIV) have all been found to activate TLR7 (18, 19, 21).

2.4: Role of TLR7 in HIV Immune Response

The main target cell of the HIV retrovirus is the CD4+ T cell, which does not express TLR7 or TLR8 (22). However, TLR7 and TLR8 are expressed on multiple cell types of the innate immune system, such as dendritic cells, macrophages, and monocytes that are also targets of HIV (66). Selective cellular expression of TLR7 and TLR8 also

occurs. For example, both TLR7 and TLR8 are expressed on B cells and monocytes,

TLR7 is expressed on both myeloid (mDC) and plasmacytoid dendritic cells (pDC), and

TLR8 is expressed on myeloid dendritic cells only (96-98). Stimulation of TLR7/8 on

these innate immune system cells by synthetic ssRNA from HIV retrovirus results in anti-

HIV activity, as demonstrated by NF-κB activation which results in the secretion of

proinflammatory and antiviral cytokines (18, 19, 66). It has also been shown that human

pDCs are activated and mature following exposure to intact HIV *in vitro* (99). Another

recent discovery is that activation of TLR7/8 results in opposing immune responses in

acute versus latent infection. Activation of TLR7/8 has been shown to block HIV

replication *in vitro* in acutely infected human aggregate lymphocyte cultures (HLAC) and

peripheral blood mononuclear cells (PBMC). Once TLR7/8 is activated, there is a

reduction of HIV co-receptor expression on CD4+ T cells. Additionally, when TLR7/8 is

triggered, an IFN-α anti-viral state is produced (22). Of the subset of cells that produce an

anti-viral state, pDCs seem most likely to be responsible, as they produce the highest

levels of anti-viral IFN-α (100-102). However, it has been shown that of the cell

population in lymphoid tissue, it is B cells that mediate the TLR7/8-dependant anti-HIV

effects, which implies a role for B cells in innate immunity. In contrast to acute infection,

TRL7/8 activation in latently infected cells results in release of HIV virions and the

activation of HIV replication in the cells of the myeloid-macrophage cell line (22).

2.5: Fr98 Retrovirus System

The group of lentiviruses that induce immunodeficiency such as HIV, SIV, FIV,

and Fr98, a polytropic murine retrovirus, all induce severe clinical CNS disease. (103-

108). Fr98 is a polytropic retrovirus and was created by combining a rapidly replicating

retrovirus (FB29) with the cloned envelope gene of an extremely neurovirulent virus (FMCF98) (107). Fr98 primarily infects CNS microglia cells, macrophages, and occasionally oligodendrocytes (108). In the brain, Fr98 produces astrogliosis, microgliosis, and mild vacuolar and neuronal degeneration (1, 107). Fr98 produces the same neurological disease and pathology as FMCF98, but CNS disease is seen 20-30 days post-infection instead of 6-8 months (108). Clinical disease consists of ataxia, hind limb weakness, tremors, seizures, and death (107). A comparative study of Fr98 and the non-neurovirulent chimeric polytropic retrovirus Fr54 demonstrated that the two viruses were very similar in that they infect the same cell types, cause similar pathology, induce no significant changes in apoptosis gene expression, and had no associated lymphocytic infiltrates (2, 109). The lack of inflammatory infiltrates implies that the innate immune response is mediating the pro-inflammatory cytokine and chemokine response. Fr98 differs, however, in that it produces a much higher viral load than Fr54 and activates astrocytes and microglia/macrophages. In Fr98 pathogenesis there is also significant gene up-regulation of pro-inflammatory cytokines and chemokines, which does not occur in Fr54 retrovirus infections. Up-regulated pro-inflammatory genes in Fr98 infection include: Tnfα, Tnfβ, Il-1α, Ccl2, Ccl3, Ccl4, Ccl5, Ccl7, Ccl12, Cxcl1, and Cxcl10 (1, 2). The structural difference between Fr98 and Fr54 that results in these differences is in the envelope protein. Currently, two neurovirulent determinants have been discovered on the Fr98 genome which appear to be mechanistically different yet complementary to each other (2, 109).

We studied the mechanism by which TLR7 contributes to neuroinflammation in the neonatal brain using a mouse model of polytropic retrovirus infection. In this mouse

model, infection of neonatal mice with the neurovirulant polytropic retrovirus, Fr98, induces severe clinical neurologic disease characterized by ataxia, seizures, and/or death by 2-3 weeks post-infection. The effects of retrovirus infection in the CNS include viral encephalitis with associated microgliosis, mild vacuolar and neuronal degeneration, astrogliosis, and minimal mononuclear cell infiltrates (1, 107). Fr98 primarily infects CNS microglial cells, macrophages, endothelial cells, and occasionally oligodendrocytes, suggesting an indirect mechanism of neuropathogenesis (107, 108). One mechanism by which Fr98 induces neuropathogenesis may be the up-regulation of pro-inflammatory cytokines and chemokines, which correlates with neuropathogenesis. In the current study, TLR7 knockout mice were used to examine the role of TLR7 in virus-mediated host neuroinflammatory responses and pathogenesis induced by Fr98 infection. We found that TLR7 had a significant impact on cytokine and chemokine induction and astrocyte activation during retrovirus infection.

Chapter 3: Materials and Methods

3.1: Solutions

10X Tris buffered EDTA (TBE)

       108 g Tris base (890 mM)

       55 g boric acid (890 mM)

       40 ml 0.5 M EDTA, pH 8.0

       Mix completely and stored at RT.

1X Tris buffered EDTA (TBE)

       100 ml 10X stock TBE

       900 ml ddH$_2$O

       Mix completely and stored at RT.

3.2: Mouse Strain

       TLR7-deficient C57BL/6 mice (89) were backcrossed with Inbred Rocky Mountain White (IRW) mice for eight generations prior to use. The *Tlr7* gene is located on the X chromosome. To generate litters of 50% TLR7+ (+/- or +) and TLR7- (-/- or -) male mice containing the *Tlr7* allele were mated with *Tlr7* heterozygous females. All mice were maintained at the Louisiana State University School of Veterinary Medicine, which is fully accredited by the Association for the Assessment and Accreditation of Laboratory Animal Care. All animal experiments were conducted in accordance with the regulations of the Louisiana State University Institutional Animal Care and Use Committee and the guidelines set forth by the National Institutes of Health.

3.3: Genotyping for Tlr7 Wild-type and Knockout Alleles

DNA was isolated from individual mouse tail biopsies using Sigma GenElute Mammalian Genomic DNA Miniprep Kit (Sigma Aldrich, St. Louis, MO). A dry heat block was preheated to 55°C and all kit reagents were thoroughly mixed by shaking. The Wash Solution was prepared by mixing 1 part Wash Solution Concentrate with 4 parts EtOH. Proteinase K was dissolved in sterile ddH$_2$O and mixed by pipetting to obtain a 20 mg/ml stock solution. One Miniprep binding column and three 2 ml collection tubes were labeled for each sample. Tail biopsies were removed from -80°C storage, and each was placed in a 1.5 ml microcentrifuge tube. To each tube, 180 µl of Lysis Solution T and 20 µl of Proteinase K solution were added to digest the tissue. The samples were then vortexed to ensure that the tail biopsies were completely submerged. The samples were incubated at 55°C on the dry heat block for 4-6 hours with hourly vortexing until completely digested. After digestion the samples were vortexed and 20 µl of RNAse A solution was added to each sample to remove residual RNA. The samples were allowed to incubate in the RNAse A solution for 2 minutes at room temperature. 200 µl of Lysis Solution C was then added to lyse the cells, and the samples were vortexed thoroughly for 15 seconds. To each Miniprep Binding Column, 500 µl of Column Preparation Solution was added and centrifuged at 12,000 x g for 1 minute to maximize the binding of DNA to the membrane. The flow-through was discarded and 200 µl of 100% EtOH was added to the lysate and vortexed for 5-10 seconds to prepare for binding. The entire contents of the tube were transferred into the treated binding column using a wide-orifice pipette tip (to reduce shearing the DNA) and centrifuged at > 6,500 x g for 1 minute. The collection tube was discarded and the binding column was placed in a new 2 ml

15

collection tube. 500 μl of the appropriately diluted Wash Solution was added to the

binding column and centrifuged at 6,500 x g for 1 minute. The Wash Solution was

necessary because the binding column must be free of ethanol before the DNA is eluted.

Once again, the collection tube was discarded and the binding column was placed in a

new 2 ml collection tube. Another 500 μl of Wash Solution was added to the binding

column and samples were centrifuged at > 16,000 x g for 3 minutes to dry the binding

column. The collection tube was discarded and the binding column was placed in a new

2 ml collection tube. Directly into the center of the binding column, 200 μl of the Elution

Solution (10 mM Tris-HCl, 0.5 mM EDTA) was added and left to incubate at room

temperature for 5 minutes to increase the elution efficiency. The samples were

centrifuged at 6,500 x g for 1 minute to elute the DNA. The binding column was

discarded and genomic DNA (gDNA) samples were stored at 4°C for short-term storage.

For analysis by PCR, gDNA samples were removed from storage and placed on

ice. A master mix was made using 8 μl of nuclease-free water, 8 μl Eppendorf$^{®}$

MasterMix 2.5x (containing: Taq DNA Polymerase (0.0625 U/μl), 125 Mm KCl, 75 mM

Tris-HCl pH 8.3, 3.75 MgCl$_2$, 0.25% Nonidet$^{®}$ -P40, 500 μM of each dNTP stabilizers),

1 μl TLR7 forward primer, 1 TLR7 reverse primer, and 1 μl TLR7 wildtype primer for

each sample run. The master mix was dispensed into tubes and the appropriate samples

were added and vortexed and quickly centrifuged. Detection of both wild-type and

knockout alleles were completed in the same PCR reaction using the *Tlr7* forward

primer: TCC AGT GTC ATG CCT ACC TGT in combination with the *Tlr7* wild-type

primer: GGC GGT CAG AGG ATA ACT TGT and the *Tlr7* knockout primer: ATG CCT

GCT TGC CGA ATA TC. Products were amplified under the following conditions: 94°C

for 3 min, followed by 25 cycles at 94°C for 30 s, 60°C for 30 s and 70°C for 30 s, and 72°C for 10 min. After the PCR reaction was completed, 5 μl Cresol red/40% Glycerol loading dye was added to sample. Samples were run on a 1.5% agarose gel which was made by adding 1.5 g agarose to 100 ml 1X TBE. The mixture was microwaved for 120 seconds at full power until the agarose had dissolved. The flask was removed, 3 μl EtBr was added and the agarose was mixed by swirling the flask. The mixture was poured into the gel caster and 26-well combs were inserted. The gel was allowed to cool. Once set, the gel was placed in the mini-gel tank and covered in 1X TBE. The combs were removed and 10 μl of the BioRad EzLoad HT Molecular Marker (Bio-Rad Laboratories, Hercules, CA) was added to the first and last lanes and 10 μl of sample were loaded into the appropriate lanes. The lid was placed on and the gel was run at 150 V for 30 minutes or until the dye was half-way down the gel. The gel was viewed on a FluorChem 8800 (Alpha Innotech, San Leandro, CA). Wild-type alleles were detected by a 250 bp band, and knockout alleles were detected by a 450 bp band. Expression of *Tlr7* mRNA correlated with the *Tlr7+/-, +* and *-/-, -* genotypes.

3.4: Virus Infection and Sample Collection

The construction of virus clone Fr98 has been previously described (107). Virus stocks were prepared from the supernatant of Fr98 or mock-infected *Mus dunni* fibroblast cell cultures. Envelope-specific monoclonal antibodies 514 and 720 were used in focus forming assays to determine virus titers (110). Virus stocks were stored at -80°C until use. Newborn IRW mice were infected intraperitoneally (i.p.) with 100 μl of cell culture supernatant containing mock virus or 10^4 focus-forming units (FFU) of Fr98 virus within 24 hours of birth using a 27 ½ gauge needle and 1 ml syringe (Becton Dickinson,

Franklin Lakes, NJ). Mice were observed daily for clinical signs of CNS disease, which include ataxia and/or seizures (107). At the onset of clinical disease or the appropriate time point, animals were euthanized under isoflurane anesthesia via exsanguination by cardiac puncture. Brains, spleens, tails, and serum were collected from each animal and flash frozen in liquid nitrogen and stored at -80°C. Prior to freezing, brains were divided in half sagittally with one half immersion-fixed in 3.7% neutral buffered formalin (NBF) for 48 hours and kept in 70% ethanol until histological processing and the other half flash frozen in liquid nitrogen and stored at -80°C for RNA isolation or multiplex analysis.

3.5: Histological Analysis

Hemisected brain tissue samples were immersion fixed in 3.7% neutral-buffered formalin for 48 h, embedded in paraffin and cut in 4-μm para-central saggital sections that included cerebrum, cerebellum, and brainstem. Tissue sections were then adhered to coated microscope slides and stained with hematoxylin and eosin (H&E) using an automated histological stainer. Additional tissue samples were stained with antibodies to virus envelope, CD3 (Dako, Carpinteria, CA), or active-caspase 3 (Promega, Madison, WI) as described below. Slides were examined in a blind fashion for histopathological evidence of neuroinflammation and neurodegeneration.

3.6: Immunohistochemistry Analysis

Sections were incubated twice in xylene for fifteen minutes to remove residual paraffin and rehydrated with five minute incubations in 100%, 95%, 70% ethanol, and twice in PBS. Antigen retrieval was performed using sodium citrate antigen retrieval buffer in a decloaking chamber (Biocare Medical, Concord, CA) set at 120°C for 20 minutes and cooled to 90°C. Pressure consistently read between 12-15 psi. When slides

reached 90°C, they were rinsed four times with ultra pure water by replacing half of the volume of antigen retrieval solution with water. Slides were then washed twice with 0.5% coldwater fish skin gelatin (Sigma Aldrich, St. Louis, MO) /PBS (0.23% FSG/PBS) for ten minutes on a rocker. Slides were incubated in a humidity chamber (Evergreen Scientific, Los Angles, CA) in 175 μl normal donkey serum blocking solution for at least 30 minutes. Slides were incubated overnight at 4°C with primary antibody. TLR7 antigen was detected using a polyclonal rabbit anti-TLR7 antibody (Zymed, Carlsbad, CA), with biotinylated goat anti-rabbit secondary antibody and streptavidin conjugated to AlexaFluor 555 (Invitrogen, Carlsbad, CA). CD31 was detected using a goat polyclonal antibody to mouse CD31 and a rabbit anti-goat antibody conjugated to AlexaFluor 488 (Invitrogen). gp70 was detected using a rabbit anti-goat IgG conjugated to AlexaFluor 555 (Invitrogen). Secondary antibodies were applied at a dilution of 6.67 μg/ml in 0.5% FSG/PBS and incubated for at least 30 minutes at room temperature. All sections were counterstained with DAPI. Slides were rinsed twice in 0.5% FSG/PBS. Slides were mounted with ProLong Gold anti-fade reagent (Invitrogen) and allowed to set for at least two hours at 4°C. An irrelevant rabbit anti-mouse Ig antibody did not produce detectable fluorescence. Images were psuedo-colored and overlayed using ImagePro Plus software.

3.7: Mutiplex Assay for Chemokine Expression

Brain tissue samples were retrieved from -80°C storage, weighed, and homogenized in 400 μl of Bio-Plex cell lysis solution (BioRad) containing Complete Mini protease inhibitors (Roche Applied Science, Indianapolis, IN) and 2 mM phenylmethylsulfonyl fluoride (Sigma Aldrich) was added. Samples were homogenized

using Kontes Disposable Pellet Pestles and a cordless motor (Fisher Scientific, Hampton, NH) and diluted to 400 μg/ml in lysis buffer. Samples were centrifuged at 4500 x g for 15 min at 4°C; cellular debris was removed and the supernatants were collected and held on ice until use. Cytokine protein expression was analyzed using a BioRad 6-plex assay (BioRad, Hercules, CA). A working wash buffer was prepared by warming the 20X concentrate to room temperature and vortexing it to remove any precipitate. 15 ml of wash buffer concentrate was mixed with 285 ml deionized water in a 500 ml media bottle. The assay diluent was prepared by diluting it with an equal volume of lysis buffer. To set up for vacuum aspiration, a plate lid was placed on the manifold (with metal grid) and the house vacuum was turned on. Then the valve was opened to the manifold and the vacuum was adjusted to less than 5" Hg. The valve to the manifold was closed and the plate lid was removed. To perform vacuum aspiration, the valve was opened to the manifold and the loaded plate was placed on the manifold. Once the aspiration was complete (< 3 seconds), the valve to the manifold was closed and the plate was removed. The bottom of the plate was blotted with a Kimwipe (Kimberly-Clark, Irving, TX) and the plate was placed on an inverted lid to load. Within an hour of use, the standard was prepared to a total volume of 1 ml. For the 6-plex standard, 1 ml of diluent was added to the vial and left to sit at room temperature for 10 minutes. Six 300 μl diluent tubes were prepared along with one 300 μl diluent blank. The standard vial was inverted to mix and then serial three-fold dilutions were performed by transferring 150 μl starting with the standard into 300 μl, then mixing, changing tips, and transferring. A plate map of samples to be run was made, and the plate was pre-wet by adding 200 μl of wash buffer to each well of the plate. The wash buffer was allowed to sit for 15-30 seconds and then vacuum

aspirated and blotted with a Kimwipe. Immediately prior to use, the 6-plex beads were

vortexed for 30 seconds and then sonicated for 30 seconds. The beads were washed by

adding 25 μl beads per well and 200 μl wash buffer to each well of the plate. The

beads/wash buffer mixture was allowed to sit for 15-30 seconds and then was vacuum

aspirated. A wash was performed by the addition of 200 μl of wash buffer, allowing the

plate to sit for 15-30 seconds, followed by vacuum aspiration. The bottom of the plate

was wiped with a Kimwipe. The standard and sample reactions were then prepared by

adding 50 μl Incubation buffer to each well. 100 μl of standard and blank were added to

designated duplicate wells, and 50 μl of appropriate assay diluent was added to sample

wells. Then 50 μl of clarified sample was added to designated duplicate wells, resulting

in a 1:2 dilution of sample. The plate was covered to protect the beads from light for the

rest of the assay and allowed to incubate at room temperature on an orbital shaker at 500-

600 rpm for 2 hours. 10-15 minutes prior to the end of the incubation, the biotinylated

detector antibody (BioRad) was prepared by diluting 1 ml of the 10X concentrate with 9

ml biotinylated detector antibody diluent (BioRad) in a non-Corning 15 ml polypropylene

conical tube. After the 2 hour incubation was complete, the plate was vacuum aspirated

and the previously described wash was repeated twice. The bottom of the plate was

wiped with a Kimwipe. 100 μl of diluted biotinylated detector antibody was added to

each well and the plate was covered and allowed to incubate at room temperature on an

orbital shaker at 500-600 rpm for 1 hour. 10-15 minutes prior to the end of the

incubation, the Strepavidin-RPE (BioRad) was prepared by diluting 1 ml of the 10X

concentrate with 9 ml Strepavidin-RPE Diluent in a foil wrapped non-Corning 15 ml PP

conical tube. The beads were then washed twice as previously described above. To each

well, 100 μl of Strepavidin-RPE was added and allowed to incubate at room temperature on an orbital shaker at 500-600 rpm for 30 minutes. The beads were then washed and vacuum aspirated three times as described above. 100-125 μl of wash buffer was added to each well and the plate was covered. Immediately prior to reading, the plate was placed on an orbital shaker at 500-600 rpm for 2-3 minutes. Cytokine protein expression was then analyzed using a Bio-Plex system instrument (Bio-Rad). Samples were calculated as pg/ml using a standard curve from in-plate standards and subsequently converted to fg/mg of brain tissue.

Table 1**:** Cytokines and Chemokines of Interest

Cytokine/Chemokine Abbreviation	Cytokine/Chemokine Full Name	Cytokine/Chemokine Function
IL-12p70	Interleukin-12	Induces INFγ production by T cells
MIP-1α	Chemokine ligand 3	Monocyte/lymphocyte attractant
MIP-1β	Chemokine ligand 4	Monocyte/lymphocyte attractant
MCP-1	Monocyte chemoattractant protein 1	Monocyte attractant
RANTES	Chemokine ligand 5	Lymphocyte attractant
TNF-α	Tumor necrosis alpha	Involved in apoptosis and cell proliferation

3.8: Preparation of RNA for Real-Time PCR analysis

Tissues were removed from storage at -80°C and transferred to a TropiCooler set at -10°C. Tissues were homogenized in 2 ml of Trizol reagent (Invitrogen), an effective inhibitor of RNase activity, in a sterile dounce homogenizer, pestle size B. The homogenate was divided into two 1.5 ml centrifuge tubes, and the homogenizer was rinsed with 1 ml of Trizol between samples. To allow for complete dissociation of nucleoprotein complexes, homogenates were left at room temperature for 5 minutes, and

then 200 μl of chloroform was added to each tube. Tubes were then shaken for 15 seconds and then incubated for 2-3 minutes at room temperature. The samples were then centrifuged at 12,000 x g for 15 minutes at 4°C in an Eppendorf table-top centrifuge to create a phenol-chloroform phase (proteins), an interphase (DNA), and an RNA containing upper aqueous phase. The aqueous phase was removed and transferred to a new 1.5 ml centrifuge tube. RNA was precipitated using 600 μl isopropanol and the samples were incubated for at least 10 minutes at room temperature. Samples were then centrifuged at 12,000 x g for 10 minutes at 4°C. The RNA precipitate formed a gel-like cloudy pellet at the bottom of the tube. The supernatant was poured off all samples, 1 ml of 70 % ethanol was added and the samples were briefly vortexed to dislodge and wash the RNA pellet. The samples were centrifuged at 7,500 x g for 5 minutes at 4°C and the ethanol was poured off. The pellets were air dried for 5-10 minutes and 50 μl of RNAse-free water was added to solubilize the pellets. The samples were incubated at 55°C for 10 minutes on a dry heat block, briefly vortexed and then centrifuged, then placed in storage at -80°C.

Following Trizol purification, all RNA samples were subsequently treated with DNase (Ambion, Austin, TX) to remove any residual genomic DNA from the purified RNA. Using the Ambion DNase I kit, a master mix was made by combining 10 μl DNase buffer, 15 μl (30 units) of DNase I, and 70 μl RNase-free water for each sample. For each RNA sample, 95 μl of the master mix was added to a clean 1.5 ml centrifuge tube and 10 μl of the appropriate sample was added. The master mix and sample were mixed by pipetting, and then briefly centrifuged and incubated at 37°C for 30 minutes, allowing the DNase I enzyme to degrade any gDNA that could result in false positive

signals in subsequent RT-PCR. Samples were then purified over Zymo RNA Cleanup

Columns (Zymo Research). To each sample, 400 µl of RNA-Binding buffer (Zymo

Research) was added, pipetted to mix, and was then transferred to a Zymo-spin column

and centrifuged for 30 seconds at full speed. The RNA, bound to the column by the

RNA-Binding buffer, was washed twice with 350 µl of Wash Buffer (Zymo Research)

and centrifuged for 30 seconds at full speed to remove Wash Buffer residues. RNA was

eluted by adding 50 µl of RNase-free water to the column and briefly centrifuging it at

>10,000 x g. The eluent was used immediately or stored at -80°C.

The RNA was reverse-transcribed to make cDNA for RT-PCR using an iScript

Reverse Transcription kit (Bio-Rad). First, a master mix was made using 10 µl nuclease-

free double distilled water, 4 µl of 5x iScript Reaction Mix, and 1 µl iScript reverse

transcriptase (iScript RT) for each sample. For the non-reverse transcribed (no-RT)

controls, 1 µl of water was used in place of the iScript RT. In a 0.5 ml tube, 5 µl of the

appropriate sample and 15 µl of the master mix were mixed together. Additionally,

control samples of RNA were made and serially diluted 1:5, 1:25, and 1:125 to measure

the efficiency and sensitivity of the reverse transcription process. The samples were then

placed in an MJ Research PTC Thermal Cycler (MJ Research Inc., Quebec, Canada) and

run under the following conditions: 25°C for 5 minutes, 42°C for 30 minutes, 85°C for 5

minutes, and held at 20°C until removed. Following the reverse transcriptase reaction,

samples were briefly centrifuged and diluted four-fold in RNase-free water. cDNA was

stored at -20°C prior to use in real-time PCR reactions.

3.9: Real-time PCR Analysis of Gene Expression

A master mix was made using 17.5 μl 2x iTaq SYBR Green Supermix with Rox (Bio-Rad), 1.75 μl of forward and reverse primers (1.8 μM final concentration) and 9 μl RNase-free H_2O for a total volume of 30 μl per sample. In a 96 well plate kept on a cooling block, 30 μl of master mix was dispensed into each well and 5 μl (10 ng) of cDNA or water was added to the appropriate well. The plate was covered with RNase/DNase-free film, vortexed to mix, and centrifuged at 1500 rpm for 5 minutes. The film was removed and the samples were dispensed 10 μl per well in triplicate into a 384 well plate (Applied Biosystems, Foster City, CA) using a Matrix electronic repeating pipette (Matrix Technologies, Hudson, NH). Once again, the plate was covered with RNase/DNase-free film and centrifuged at 1500 rpm for 5 minutes. Plates were kept at 4^oC until analysis on an ABI PRISM 7900 Sequence Detection System (Applied Biosystems). Primers for real-time PCR analysis are shown in Table 2. All primers used for real-time analysis were designed using Primer3 software (111). To confirm that all primer pairs were specific for the gene of interest and that no homology to other genes was present, primers were compared against the National Center for Biotechnology Information (NCBI) website. Analysis of dissociation curves was used to confirm the amplification of a single product for each primer pair per sample. Confirmation of a lack of DNA contamination was achieved by running reactions without reverse transcriptase. Untranscribed controls had at least a 1000-fold lower expression level than analyzed samples or were negative for all genes after 40 cycles. Gene expression was quantified by the cycle number at which each sample reached a fixed fluorescence threshold (C_T). To control for variations in RNA amounts among samples, data were calculated as the

difference in C_T values ($\log_2$) between *Gapdh* and the gene of interest for each sample

($\Delta C_T = C_T$ Gapdh $- C_T$ gene of interest). Therefore, data are presented as a percentage of

Gapdh expression for each gene of interest.

3.10: Statistical Analysis

All statistical analyses were performed using Graph-Pad Prism software (San Diego, CA)

using the appropriate statistical test as stated in each figure legend. Indications of

statistical significance are: * = $p < 0.05$, ** = $p < 0.01$, *** = $p < 0.001$.

Table 2. List of primers used for real-time PCR analysis.

Common gene Name	NCBI Gene Symbol & ID#	Forward primer	Reverse Primer
Actin	*Actb*: 11461	CAGCTTCTTTGCAGCTCCTT	CACGATGGAGGGGAATACAG
CD3 antigen epsilon	*Cd3e*: 12501	GAGCACCCTGCTACTCCTTG	TGAGCAGCCTGATTCTTTCA
Chemokine ligand 2 (MCP-1)	*Ccl2*: 20296	TCCCAATGAGTAGGCTGGAG	CCTCTCTCTTGAGCTTGGTGA
Chemokine ligand 3 (MIP-1α)	*Ccl3*: 20302	ACCATGACACTCTGCAACCA	GATGAATTGGCGTGGAATCT
Chemokine ligand 4 (MIP-1β)	*Ccl4*: 20303	AGTCCCAGCTCTGTGCAAAC	CCACGAGCAAGAGGAGAGAG
Chemokine ligand 5 (RANTES)	*Ccl5*: 20304	GGTTTCTTGATTCTGACCCTGTA	AGGACCGGAGTGGGAGTAG
Chemokine ligand 10 (IP10)	*IP10*: 15945	CAGTGAGAATGAGGGCCATAGG	CTCAACACGTGGGCAGGAT
Friend murine leukemia virus Fb29 gag (gag)	gag: 1491876	AAACCAATGTGGCCATGTCATT	AAATCTTCTAACCGCTCTAACTTTCG
F4/80	*Emr1*: 13733	TTACGATGGAATTCTCCTTGTATATCA	CACAGCAGGAAGGTGGCTATG
Glyceraldehyde-3-phosphate dehydrogenase (Gapdh)	*Gapdh*: 407972	TGCACCACCAACTGCTTAGC	TGGATGCAGGGATGATGTTC
Glial fibrillary acidic protein (GFAP)	*Gfap*: 14580	CGTTTCTCCTTGTCTCGAATGAC	TCGCCCGTGTCTCCTTGA
Integrin alpha X (Cd11c)	*Cd11c*: 16411	ATGTTGGAGGAAGCAAATGG	TGGGGCTGACTTAGAGGAGA
Interferon beta (Ifnb1)	*Ifnb1*: 15977	AGCACTGGGTGGAATGAGAC	TCCCACGTCAATCTTTCCTC
Myeloid differentiation primary response 88 (MyD88)	*Myd88*: 17874	CATGGTGGTGGTTGTTTCTG	CTGTTGGACACCTGGAGACA
Toll-like receptor 3	*Tlr3*: 142980	AGCTTTGCTGGGAACTTTCA	ATCGAGCTGGGTGAGATTTG
Toll-like receptor 4	*Tlr4*: 21898	GGCAGCAGGTGGAATTGTAT	AGGATTCGAGGCTTTTCCAT
Toll-like receptor 7	*Tlr7*: 170743	GGCATTCCCACTAACACCAC	TTGGACCCCAGTAGAACAGG
Toll-like receptor 8	*Tlr8*: 170744	TCGTCTTGACCATTTGTGGA	AATGCTCCATTTGGGATTTG
Toll-like receptor 9	*Tlr9*: 81897	ACTTCGTCCACCTGTCCAAC	TCATGTGGCAAGAGAAGTGC
Tumor necrosis factor alpha	*Tnf*: 21926	CCACCACGCTCTTCTGTCTAC	GAGGGTCTGGGCCATAGAA

Chapter 4: Results

4.1 Effect of TLR7 Deficiency on Fr98-induced Neurologic Disease

To analyze the role of TLR7 in neuropathogenesis, TLR7+ and TLR7- littermates were infected i.p. with Fr98 or mock culture supernatants within 24 hours of birth and followed for the development of clinical disease. No significant difference in the development of neurologic disease was observed in TLR7- mice versus TLR7+ mice (Fig. 3). Additionally, there were no notable distinctions in the histopathology of Fr98-infected TLR7+ and TLR7- mice as detected in hematoxylin and eosin (H&E) stained sections or in tissue sections stained with antibodies to CD3, viral envelope protein or active caspase 3 (data not shown). Thus, TLR7 did not appear to play a critical role in the development of Fr98-mediated neurologic disease.
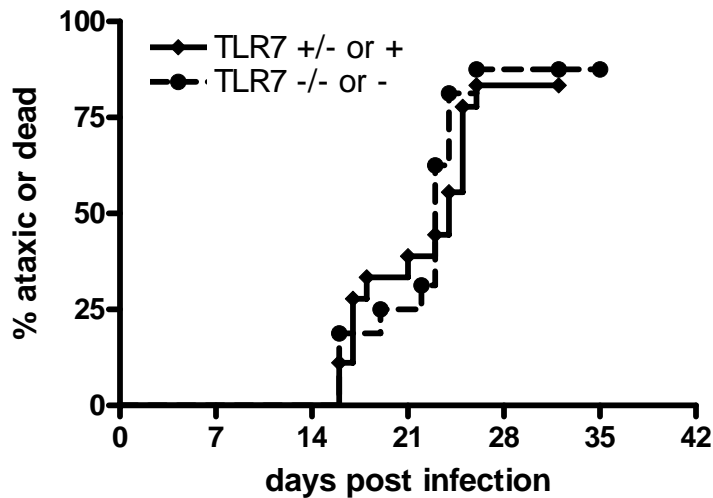
Figure 3. Analysis of the effect of TLR7 deficiency on neurologic disease. Development of neurologic disease in TLR7 positive (+/- or +) and TLR7 deficient (-/- or -) Fr98-infected mice and age-matched control mice. At the time of clinical disease, mice were genotyped for *Tlr7* positive and knockout alleles. Data are presented as the percentage of mice (14 TLR7- mice and 15 TLR7+ mice) with severe ataxia or death. Data was analyzed using Kaplan-Meir survival curve and log-rank post-test.

28

4.2 Effect of TLR7 on Viral Replication, TLR8, TLR9, and the MyD88 Signaling Pathway in the Brain

To determine if TLR7 alters virus replication during infection, we analyzed brain tissue from mock and Fr98-infected TLR7+ and TLR7- mice for expression of virus gag RNA at 14 dpi, just prior to the development of clinical neurologic disease. No significant difference was observed in viral gag RNA expression in the brains (Fig. 4A) of Fr98-infected TLR7+ or TLR7- mice. Thus, TLR7-deficiency did not appear to influence virus replication in the brain.

As expected, the presence of TLR7 was demonstrated by mRNA expression in both the TLR7+ mock and Fr98 infected mice, and absent in both groups of TLR7- mice (Fig. 4B). Since TLR7, TLR8, and TLR9 comprise a subfamily in which all are confined to the membranes of endosomes and recognize similar molecular structures, the oligonucleotide-based PAMPs, we analyzed *Tlr8* and *Tlr9* mRNA expression to determine if any cooperative interactions among these receptors existed. A significant up-regulation of *Tlr8* mRNA by Fr98 infection was observed in both TLR7+ as well as TLR7- mice (Fig. 4C). An approximate 3-fold increase was observed with *Tlr9* expression in Fr98-infected TLR7+ mice compared to controls, although expression levels varied substantially between mice, making the increase not statistically significant (Fig. 4D). This increase was not observed in TLR7- mice (Fig. 4D). Additionally, we examined the mRNA expression of *Myd88*, as it is the cytosolic adaptor protein responsible for intracellular signaling initiation of TLR7, TLR8, and TLR9 (54, 55). No significant difference was seen in *Myd88* mRNA expression in the brain. Thus, multiple members of the TLR9 family of receptors were up-regulated by Fr98 infection in

wildtype mice. TLR7 deficiency may have an impact on TLR9 expression, but the

variability of TLR9 expression makes this difficult to determine.
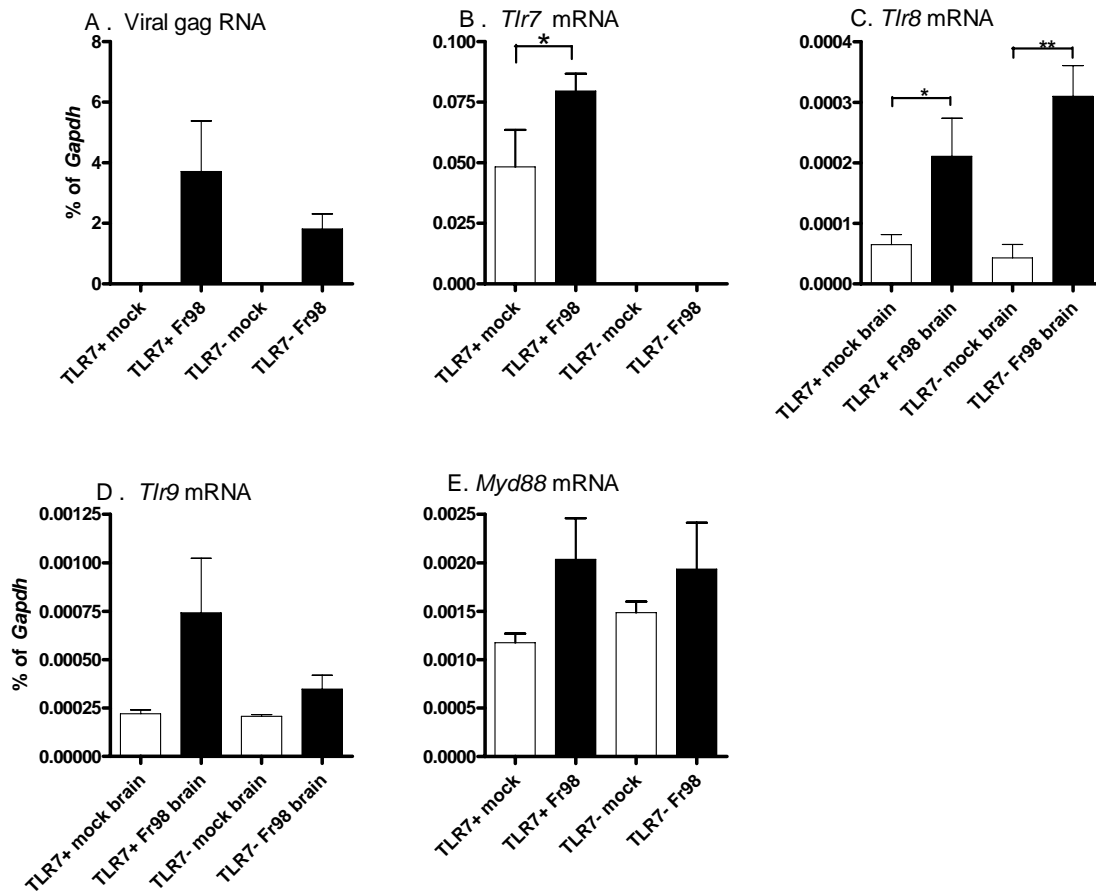
Figure 4. Analysis of the effect of TLR7 on viral replication, TLR8, TLR9, and the MyD88 signaling pathway in the brain. Brain tissue from mock and Fr98-infected mice was removed at 14 dpi, divided into two sagittal sections, snap frozen in liquid nitrogen and processed for RNA. Real-time quantitative RT-PCR analysis was performed using primers specific for (A) virus gag, (B) *Tlr7* (C) *Tlr8* (D) *Tlr9* (E) *Myd88*. Data was calculated as gene expression relative to *Gapdh* expression (% of *Gapdh* expression) for each sample. Data are the mean +/- SEM for 5-6 mice per group. Data shown is from one of two replicate experiments. Data analyses of TLR8 and TLR9 for both replicate experiments was completed at the same time and were combined for graphing and analysis. Statistical analysis was completed using a One-way ANOVA with Newman Keuls post-test analysis. * = p<0.05, ** p<0.01.

4.3 Effect of TLR7 Deficiency on Fr98-induced Cytokine and Chemokine Production by Multiplex Analysis and Real-time Polymerase Chain Reaction

Fr98 infection of neonates induces substantial innate immune responses in the brain including the production of proinflammatory cytokines as detected by both mRNA and protein expression (1, 107, 108, 112, 113). To determine the role of TLR7 in the innate immune response to Fr98 infection, brain tissue was analyzed for proinflammatory cytokines and chemokines by multiplex bead array. Similar to previous reports, Fr98 infection of TLR7+ mice induced a significant up-regulation of CCL2 (MCP-1), CCL4 (MIP-β), and CCL5 (RANTES) protein levels (Fig. 5A-C) (1, 2). CCL3, TNF and Il-12p70 protein levels were below sensitivity levels by multiplex bead array (data not shown). In contrast to TLR7+ mice, only CCL5 protein was up-regulated significantly by Fr98-infection in TLR7- mice (Fig. 5C). However, CCL5 expression was significantly lower in TLR7- mice compared to TLR7+ mice (Fig. 5C). Thus, TLR7 appeared to play a non-redundant role in the induction of multiple pro-inflammatory chemokines during retrovirus infection in the CNS.

Since some protein levels were too low for detection, we also analyzed gene expression in the brain by real time polymerase chain reaction. Significant up-regulation of *Ccl3 (MIP-α)*, *Cxcl10 (IP-10)*, *Tnf (TNFα)* and *Ifnb1* mRNA levels were detected in the brain of Fr98-infected wildtype mice at 14 dpi (Fig. 6A-C). TLR7 appeared to be required for induction of *Cxcl10* and *Tnf* mRNA, but was not necessary for *Ccl3* or *Ifnb1* mRNA up-regulation (Fig. 6A, 6D).

A. CCL2 (MCP-1) protein

B. CCL4 (MIP-1β) protein

C. CCL5 (RANTES) protein
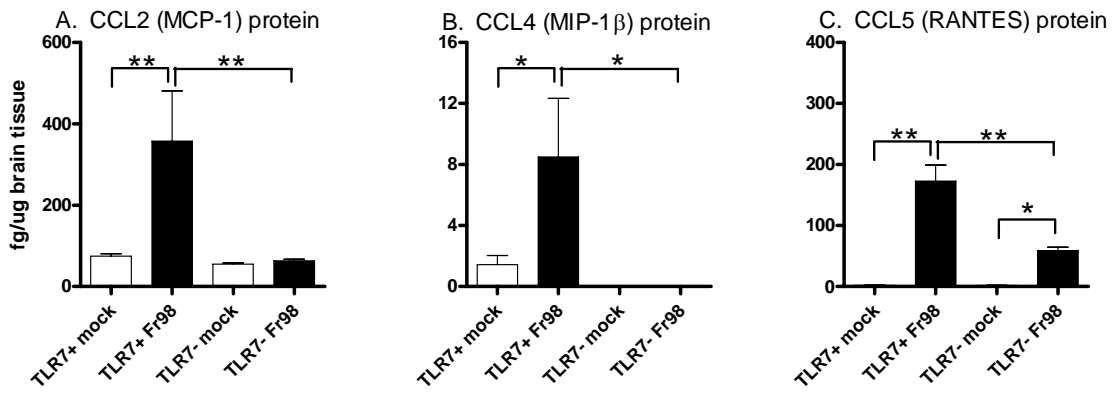
Figure 5. Influence of TLR7 deficiency on Fr98-induced cytokine and chemokine (A-C) protein levels in the brain. Brain tissue from mock and Fr98-infected mice was removed at 14 dpi, snap frozen and processed for multiplex bead array. Analysis of (A) CCL2, (B) CCL4 and (C) CCL5 protein levels in brain tissue. Results are the mean +/- standard error of 5-6 mice per group. Statistical analysis was done by One-way ANOVA with Newman Keuls post-test analysis. Statistical significance: * = p < 0.05, ** = p < 0.01.

A. *Ccl3 (MIP-1α)* mRNA

B. *Cxcl10 (IP-10)* mRNA

C. *Tnfa* mRNA

D. *Ifnb1* mRNA
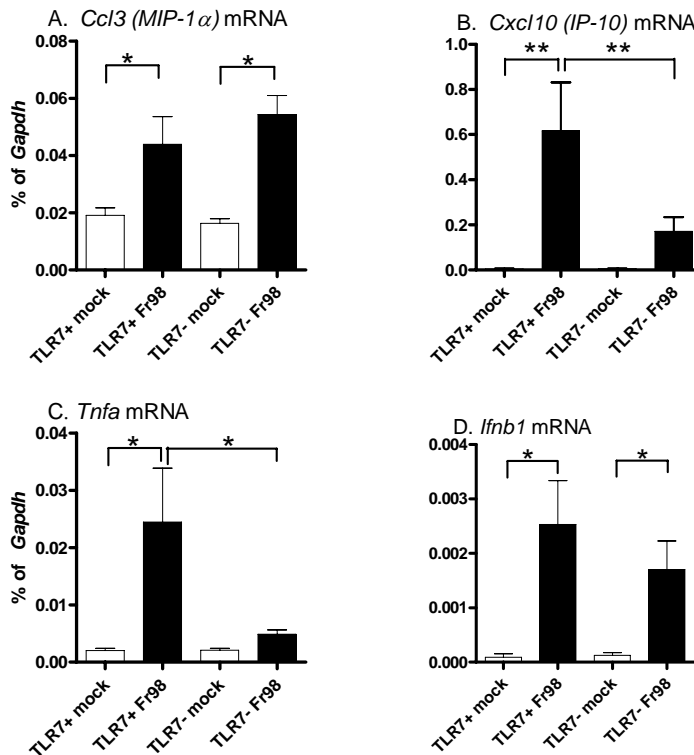
Figure 6. Influence of TLR7 deficiency on Fr98-induced cytokine and chemokine (A-D) mRNA levels in the brain. Brain tissue from mock and Fr98-infected mice was removed at 14 dpi, snap frozen and processed for real-time PCR analysis. Expression of (A) *Ccl3* (B) *Cxcl10* (C) *Tnfa* and (D) *Ifnb1* mRNA. Data shown are the gene expression as a percent of *Gapdh* mRNA expression for each sample. Results are the mean +/- SEM of 5-6 mice per group. Data shown is from one of two replicate experiments. Statistical analysis was done by One-way ANOVA with Newman Keuls post-test analysis. Statistical significance: * = p < 0.05, ** = p < 0.01.

4.4 Effect of TLR7 on Peripheral Viral Replication and TLR7 Deficiency on Fr98-induced Peripheral Cytokine Production

To investigate if TLR7 alters virus levels and cytokine production in the periphery, we analyzed splenic tissue from mock and Fr98 infected TLR7+ and TLR7- for expression of virus gag RNA at 14 dpi. No significant difference was observed in viral gag RNA expression in the spleen (Fig. 7A) between Fr98-infected TLR7+ and TLR7- mice. Thus, TLR7-deficiency did not appear to influence peripheral virus replication.
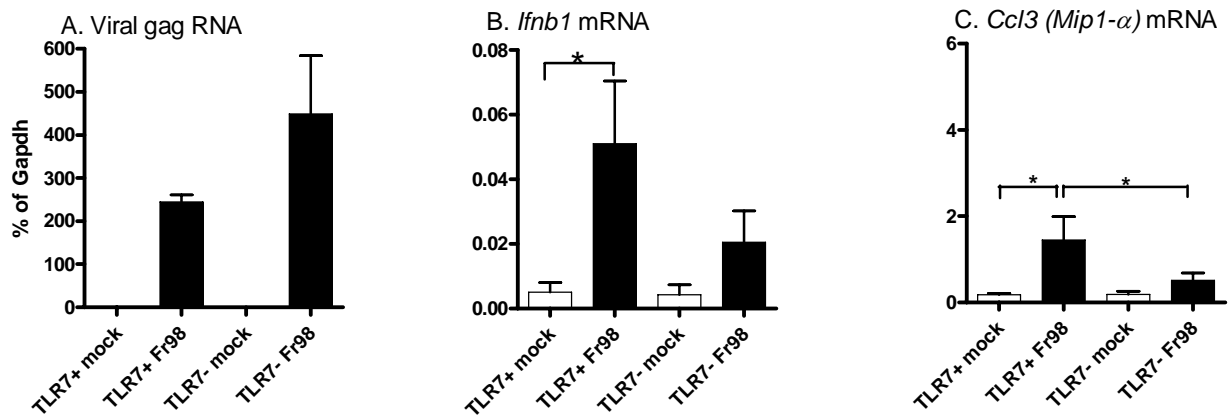
Figure 7. Expression of virus gag (A), *Ifnβ1* (B), and *Ccl3* (C) mRNA in the spleen of mock and Fr98-infected TLR7 positive and TLR7 deficient mice at 14 dpi. Splenic tissue from mock and Fr98-infected mice was removed at 14 dpi, snap frozen and processed for real-time PCR analysis. Data are the mean +/- SEM of 5-6 mice per group. Data shown is from one experiment. Statistical analysis was completed using One-way ANOVA Newman Keuls post-test analysis. Statistical significance: * = $p < 0.05$.

In the spleen, mRNA for several cytokines including *Ccl2* (*MCP-1*), *Ccl4* (*MIP-β*), *Ccl5* (*RANTES*), *Ccl3* (*MIP-α*), *Cxcl10* (*IP-10*), and *Tnf* (*TNFα*) were up-regulated in Fr98-infected TLR7+ mice compared to mock-infected controls (data not shown). Of these cytokines, only *Ccl3* mRNA was not up-regulated by Fr98 in TLR7- mice (Fig. 7C). Fr98-induced *Ifnb1* mRNA expression was lower in TLR7 deficient mice compared

to wildtype controls, but not to a significant level (Fig. 7B). Thus, TLR7 only had a limited role in peripheral immune responses to Fr98 infection.

4.5 Effect of TLR7 Deficiency on Fr98-induced Neuroinflammation

Activation of astrocytes, microglial cells, and macrophages is one of the primary pathologic changes associated with Fr98 infections (107, 108). To examine if TLR7 was involved in Fr98-induced activation of astrocytes and/or microglia/macrophages, we analyzed TLR7+ and TLR7- mice at 14 dpi for mRNA expression of *Gfap* and *F4/80* via quantitative RT-PCR. GFAP and F4/80 are up-regulated on astrocytes and microglia/macrophages, respectively, following activation (114-116). A significant increase in *Gfap* and *F4/80* mRNA expression was observed in Fr98-infected TLR7+ mice when compared to mock infected mice (Fig. 8A-B). However, *Gfap* and *F4/80* were not up-regulated in TLR7- mice (Fig. 8A-B). The pattern of GFAP staining observed by immunohistochemistry was inconclusive (data not shown).

To examine if TLR7 was involved in Fr98-induced up-regulation of other cellular molecules, we also analyzed TLR7+ and TLR7- mice at 14 dpi for mRNA expression of *Cd3ε*, *Cd11c* and *Siglec-H* via quantitative RT-PCR. *Cd3ε* is expressed by T cells, *Cd11c* is expressed by a number of cell types including dendritic cells, and *Siglec-H* is expressed by plasmacytoid dendritic cells. A significant increase in *Cd3ε* and *Cd11c* mRNA expression was observed in Fr98-infected TLR7+ mice as compared to mock infected mice (Fig. 8C-D). Additionally, *Cd3ε* and *Cd11c* mRNA was not up-regulated in TLR7- mice. No increase in mRNA expression was observed for *Siglec-H* in Fr98-infected TLR7+ or TLR7- mice (data not shown). Thus, *Cdllc* mRNA expression may be due to microglial cells which up-regulate this molecule on activation, rather than

recruitment of plasmacytoid dendritic cells which could migrate to the CNS in response to infection.
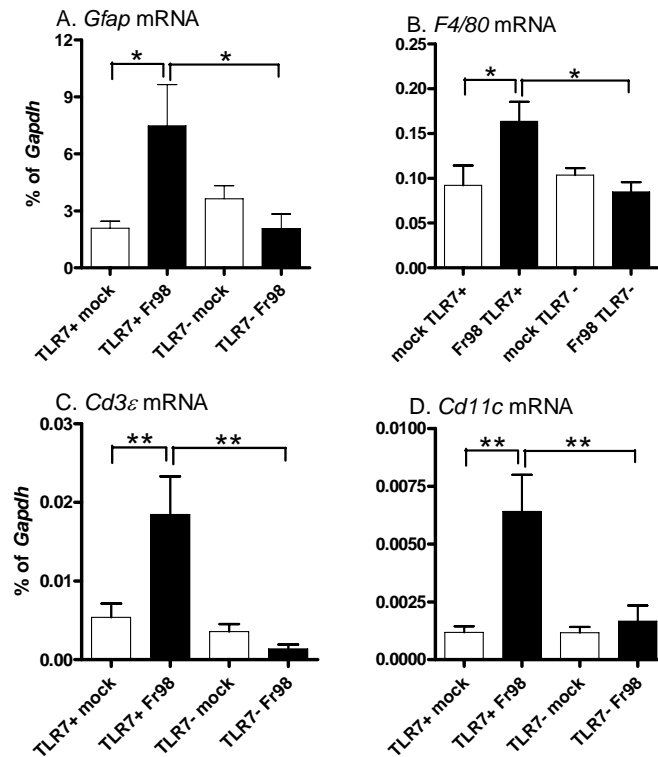
Figure 8. Expression of *Gfap* (A), *F480* (B) *Cd3ε* (C), and *Cd11c* (D) mRNA in the brain of mock and Fr98-infected TLR7 positive and TLR7 deficient mice at 14 dpi. Tissue was processed as described in Fig. 4. Real-time quantitative RT-PCR analysis was performed using primers specific for *Gfap*, *F480, Cd3ε, Cd11c*, and *Gapdh*. Data are shown as the gene expression as a percent of *Gapdh* mRNA expression for each sample. Results are the mean +/- SEM of 5-6 mice per group. Data shown is from one of two replicate experiments. Statistical analysis was done by One-way ANOVA with Newman Keuls post-test analysis. Statistical significance: * = $p < 0.05$, ** = $p < 0.01$

4.6 Effect of TLR7 on Viral Replication and the Effect of TLR7 Deficiency on Fr98-induced Neuroinflammation in Clinically Ill Animals

While we found that virus replication prior to clinical disease was not TLR7 dependent, we wanted to determine if TLR7 alters virus replication during active clinical disease. To determine this, we analyzed brain tissue from mock and Fr98 infected TLR7+ and TLR7- mice for expression of virus gag RNA when mice began to exhibit clinical signs (ataxia, seizures). No significant difference was observed in viral gag RNA

expression in the brain (Fig. 9A) of Fr98-infected TLR7+ and TLR7- mice. Thus, TLR7

deficiency did not appear to influence virus replication in the brain of preclinical or

clinically ill animals.

Since GFAP and F4/80 up-regulation was decreased in TLR7- mice in pre-clinical

animals, we analyzed *Gfap* and *F4/80* mRNA expression in TLR7+ and TLR7- mice to

determine if this remained true in clinically ill animals. Surprisingly, a significant

increase in *Gfap* mRNA expression was observed in both Fr98-infected TLR7+ and

TLR7- mice as compared to mock infected mice (Fig. 9B). No up-regulation of *F4/80*

was observed at the time of clinical disease in either Fr98-infected TLR7+ or TLR7- mice

(Fig. 9C). Thus, TLR7 appears to play a role in stimulating astrocytes early in infection

(prior to day 14), but other mechanisms appear to compensate for the lack of TLR7 at

later stages of disease.
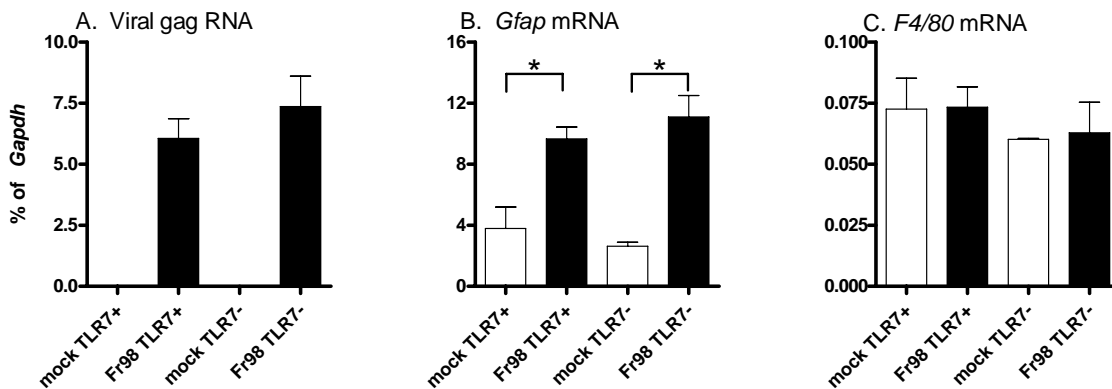
Figure 9. Expression of virus gag (A), *Gfap* (B), and *F4/80* (C) mRNA in the brain of Fr98-infected TLR7 positive and TLR7 deficient mice and age-matched controls at the time of apparent clinical disease (tremors, ataxia, seizures). Tissue was processed as described in Fig. 4. Data are the mean +/- SEM of 7-8 mice per clinical disease group and 3 mice per age-matched control group. Data shown is from one experiment. Statistical analysis was completed using One-way ANOVA with Newman Keuls post-test analysis. Statistical significance: * = $p < 0.05$.

4.7 Effect of TLR7 Deficiency on Fr98-induced Cytokine and Chemokine Production in Clinically Ill Animals

As *Gfap* mRNA was up-regulated in clinically ill TLR7- mice, we were interested in whether other inflammatory markers were also up-regulated during the clinical stage of disease. *Tnf* mRNA expression was significantly up-regulated by Fr98-infection in TLR7+ mice, but was not up-regulated by Fr98-infection in TLR7- mice (Fig. 10F).
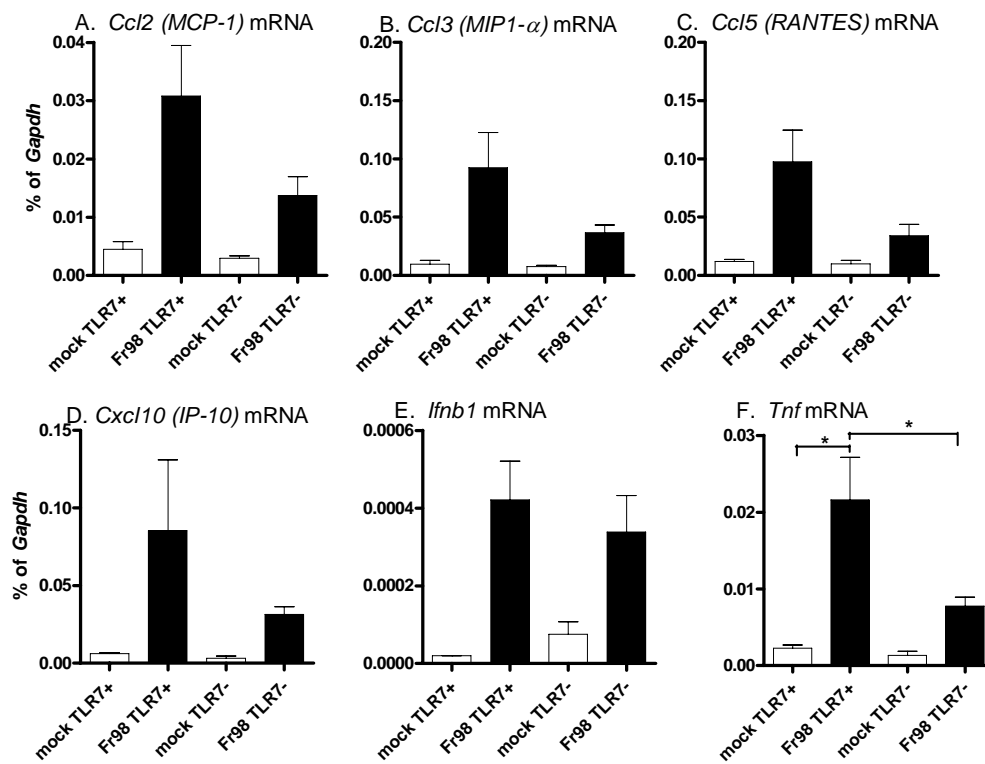
Figure 10. Influence of TLR7 deficiency on Fr98-induced cytokine and chemokine mRNA levels in the brain. Expression of *Ccl2* (A), *Ccl3* (B), *Ccl5* (C), *Cxcl10* (D), *Ifnb1* (E), and *Tnfa* (F) mRNA in the brain of Fr98-infected TLR7 positive and TLR7 deficient mice and age-matched controls at the time of apparent clinical disease (tremors, ataxia, seizures). Tissue was processed as described in Fig. 4. Data are the mean +/- SEM of 7-8 mice per diseased group and 3 mice per age-matched control group. Data shown is from one experiment. Statistical analysis was completed using One-way ANOVA with Newman Keuls post-test analysis. Statistical significance: * = p < 0.05.

For the other genes of interest, mRNA expression fluctuated too much to establish significance; however, there was an observable trend of a more substantial increase of cytokine and chemokine mRNA expression in the brain of clinically ill Fr98-infected TLR7+ animals compared to Fr98-infected TLR7- mice (Fig. 10A-D). TLR7 appeared to contribute to the induction of most cytokines and chemokines but had no effect on *Ifnb1* mRNA expression (Fig. 10E). Thus, TLR7 may play a role in modulating the innate immune response in both early and late stages of virus infection, with the exception of *Ifnb1*.

Chapter 5: Discussion

In the current study, TLR7 deficiency did not alter retroviral pathogenesis, but did alter neuroinflammation, including astrocyte activation and chemokine production. Thus, TLR7 appears to play an important role in the early glial response to retrovirus infection, and inhibition of the pathway may reduce neuroinflammation. To date, this is the first demonstration of the necessity of TLR7 for innate immune responses to retrovirus infection *in vivo*. Additionally, these results indicate that the innate immune response to retrovirus in the CNS may not be an essential step in the pathogenesis of the disease.

TLR7 stimulation has been shown to both suppress and enhance HIV virus replication in PBMC (22). In this study, TLR7 deficiency did not alter virus replication in the brain or in the spleen of pre- or post-clinically diseased mice as measured by virus gag RNA expression (Fig. 4A, 7A, 9A). This lack of an effect may be due to the immaturity of the immune system in neonates. B cells play an important role in TLR7 mediation of HIV viral replication, and these responses are not fully developed in the neonate. Additionally, spread of Fr98 may be restricted in the absence of an anti-viral response. Unlike ecotropic retroviruses which infect microglia/macrophages throughout the brain, polytropic retrovirus infection has a limited spread to microglia/macrophages around blood vessels in the thalamus, hippocampus, corpus collosum, and cerebellum (107). Thus, even in the absence of an anti-viral response, the spread of polytropic viruses may be limited.

The lack of virus spread in TLR7 deficient animals may also be due to the production of interferon beta. *Ifnb1* mRNA was up-regulated in response to retrovirus

infection in both TLR7 sufficient and deficient mice in the brain and the spleen of

animals prior to onset of clinical signs as well as in the brains of mice that exhibited

clinical signs of disease (Fig. 6D, 7B, 10E). Type 1 interferons, such as IFNβ, are

known to suppress the spread of the virus to uninfected cells (18, 19, 78, 79, 117). As

IFNβ up-regulation is a common downstream effect of TLR stimulation (69), it is

probable that stimulation of other TLR molecules are responsible for the *Ifnb1* up-

regulation observed in the TLR7 deficient mice (Fig. 6D, 7B, 10E). For example, TLR4

has been shown to be activated by retroviral glycoproteins and can induce the expression

of *Ifnb1* mRNA (118-122). Thus, TLR4 stimulation by Fr98 envelope proteins may be

sufficient for the induction of *Ifnb1* mRNA in the absence of TLR7.

Despite the lack of effect on virus replication and clinical disease in this model,

TLR7-deficiency had a significant impact on neuroinflammatory responses. Many, but

not all, chemokines were reduced and cellular responses were also limited in both the

brain and in the periphery (Fig. 5A-C, Fig. 6A-D, Fig. 7B-C). Similar suppression of the

innate immune response was observed with TLR2 deficient mice following HSV-1

infection (14). Mice deficient in TLR3 had reduced infiltration of virus and immune cells

to the brain following West Nile virus infection (123). Thus, specific TLRs may play a

critical non-overlapping role in the initiation of immune responses to certain viruses. This

effect may be more profound in the developing brain, where limited immune cell

interaction reduces the possible mechanisms available for stimulation of immune

responses.

Another factor potentially influencing the neuroinflammatory responses observed

in the study is the cooperative interactions of the TLR7, TLR8, and TLR9 (TLR7/8/9)

subfamily. Selective expression of murine TLR7, TLR8, and TLR9 in HEK293 cells has demonstrated that co-expression of TLR8 or TLR9 inhibited TLR7 activation and cytokine production (124). It is possible that selective activation and suppression within the TLR7/8/9 subfamily provides a more tailored immune response to a specific pathogen. In this study, both *Tlr8* and *Tlr9* mRNA appear to be up-regulated in TLR7+ Fr98-infected mice, with a statistical increase in *Tlr8* mRNA expression (Fig. 4C-D). However, only *Tlr8* mRNA appeared to be up-regulated in TLR7 deficient Fr98-infected mice. The observed up-regulation of *Tlr8* mRNA in TLR7- mice may indicate that *Tlr8* mRNA expression is not dependant on TLR7. The apparent lack of up-regulation of *Tlr9* mRNA expression in TLR7- mice suggests that *Tlr9* up-regulation may be dependent on TLR7 stimulation: TLR7 agonist stimulation did induce *Tlr9* mRNA up-regulation in an astrocyte cell line (data not shown), suggesting a possible self-regulatory mechanism for TLR7-induced responses.

Murine TLR8 was previously thought to be dysfunctional, based on the lack of response of murine TLR7 deficient cells to viral ssRNA stimulation and TLR7/8 agonist stimulation (125, 126). However, murine TLR8 is expressed on the embryonic and neonatal brain and has been shown to play a role in regulating axonogenesis in the developing nervous system and to inhibit neurite outgrowth and induce neuronal apoptosis, *in vit*ro (127). Possibly, TLR8 stimulation on neurons contributes to Fr98-induced pathogenesis even in the absence of other inflammatory stimuli.

Differences and similarities in stimulation and signaling within the TLR7/8/9 subfamily may also influence inflammatory responses. As previously mentioned, ssRNA genomes such as vesicular stomatitis virus, influenza A virus, and synthetic RNA

oligonucleotide from HIV have all been found to activate TLR7 (18, 21) while TLR9 recognizes dsDNA genomes such as herpes simplex virus and murine cytomegalovirus (64, 65, 79, 79). Additionally, it has been shown that during HIV infection, HIV-1 RNA, not DNA retrotranscripts, appears to be essential for activating pDCs. However, retroviruses, including HIV-1, may signal through both TLR7 and TLR9 (128). Possibly, TLR9 is being stimulated by Fr98 viral CpG DNA fragments that have been released into the cellular environment by infected apoptotic cells. Therefore, the neuroinflammatory response observed in Fr98-infected mice may be due to multiple TLR stimulation, not solely TLR7.

Due to their location, both TLR7 and TLR9 require endosomal acidification for stimulation. It has recently been shown that for plasmacytoid dendritic cell activation and subsequent IFNα production, TLR7 viral recognition and stimulation in pDCs requires transport of viral replication intermediates into the lysosome by autophagy (129). Because murine leukemia viruses may release their RNA into the cytosol (130), stimulation of TLR7 may be through autophagy of infected cells or by uptake of cellular/viral debris.

The requirement for TLR7 in Fr98-mediated up-regulation of multiple cytokines and chemokines is interesting, as many of these cytokine and chemokine-producing cells are not productively infected with virus. For example, *Ccl2* and *Cxcl10* mRNA is produced by astrocytes (112), while *Ccl3* and *Ccl5* mRNA is produced by uninfected cell types (131) (data not shown). The lack of cytokine and chemokine production correlated with the lack of activation marker expression by astrocytes. As astrocytes are not productively infected by Fr98, it is unclear how TLR7 influences their response to virus

infection. Possibly, these cells are not directly activated through TLR7 signaling, but are responding to a secreted cytokine or other signaling molecule produced by an infected cell. This response may be inhibited in the absence of TLR7. Alternatively, astrocytes and other uninfected cell types may take up viral particles including viral ssRNA by phagocytosis or pinocytosis, leading to the activation of these cells through TLR7.

TLR7, TLR8, and TLR9 are expressed on lymphoid cellular subsets: B cells and monocytes express TLR7 and 8, while pDC express TLR7 and TLR9, and CD11c immature DC only express TLR8 (96, 132-134). A significant lack of mRNA expression of *Cd3ε* and *Cd11c* in Fr98-infected TLR7 deficient versus Fr98-infected TLR7+ mice was also observed in this study, indicating that activation of T cells and dendritic/moncyte/macrophage cells is TLR7 dependent. No mRNA up-regulation was observed in the expression of *Siglec-H*, a marker for pDCs, in Fr98-infected wildtype or TLR7 deficient mice (data not shown), indicating that the cell types affected by TLR7 deficiency were mDC, monocytes or macrophages.

While TLR7 deficient mice sacrificed before clinical disease development displayed significantly reduced expression by astrocytes and microglia/macrophages compared to wildtype animals, mice which exhibited clinical signs of disease showed no difference in *Gfap* mRNA up-regulation between Fr98-infected TLR7+ and TLR- mice. Thus, TLR7 activation may stimulate astrocytes prior to the development of clinical signs, but other mechanisms appear to compensate for the lack of TLR7 during later stages of infection.

While not statistically significant (with the exception of TNF), mice which developed clinical signs of disease displayed similar innate immune responses to those

sacrificed prior to the development of clinical disease at day 14 and the peak time

increase in cytokine and chemokine expression (1) (Fig. 10A-F). The variability of

cytokine and chemokine gene expression in Fr98-infected TLR7+ clinically ill mice was

surprising as we have previously shown that cytokine and chemokine expression is

significantly and repeatedly up-regulated following Fr98-infection in wildtype IRW mice.

The variability in gene expression in this experiment could be due to multiple reasons

including the variation in the age of the mice when they developed clinical signs (13-37

dpi) and the potential influence of heterozygosity (all females +/-, all males +) of the

genotype. Additionally, these studies were completed on mice that had only been

backcrossed for eight generations, not the full ten generations required for the residual

amount of unlinked donor genome in the strain to fall below 0.01 %. While each of the

effects may be minor, the combination may be sufficient to account for the variability

observed in the cytokine and chemokine results in the wildtype mice. That withstanding,

there was still a substantial up-regulation of cytokines and chemokines in wildtype mice

following Fr98-infection, but not in knockout mice.

The lack of a strong innate immune response to Fr98 infection in TLR7 deficient

mice is also interesting in light of potential mechanisms of neuropathogenesis. The

development of clinical disease by the TLR7 deficient mice indicates that the induction

of several components of the innate immune response is not essential for

neuropathogenesis. We have previously shown that TNFa and CCL2, two of the

molecules not induced in the TLR7 deficient mice, contribute to but are not necessary for

Fr98-mediated neurologic disease (2, 112). Possibly, the absence of both TNFa and

CCL2 negates the pathogenic and protective properties of both molecules. Although we

did not observe any notable change in histopathology between Fr98-infected TLR7+ and TLR7- mice, it is possible that other molecules were up-regulated in the TLR7 deficient mice and that they contributed to disease pathogenesis, effectively compensating for the lack of TLR7. It is also probable that the innate immune response may play a more important role in slower developing neurologic disease compared to the rapid onset of pathologic changes following Fr98 infection.

In the current study, TLR7 deficiency did not alter virus replication, clinical disease, or influence the production of IFNβ1 in the brain. However, TLR7 deficiency did alter neuroinflammation, including astrocyte activation and chemokine production. Therefore, TLR7 appears to play an important role in the early glial response to retrovirus infection, and inhibition of the pathway may reduce neuroinflammation. To further define the role of TLR7 in neuropathogenesis, the neuroinflammatory and neuropathogenic properties of the TLR7/8/9 family should be evaluated, as well as how the interactions between TLR7, TLR8, and TLR9 elicit those responses. Additionally, since it has been shown in this study that TLR7 has a non-redundant role in the induction of neuroinflammatory responses in the CNS, it would be interesting to determine if the roles of TLR7 and TLR9 are pathogenic or protective during retrovirus infection in the neonatal brain. It would also be invaluable to determine how different TLR7, TLR8, and TLR9 agonists affect the innate and adaptive immune responses to retrovirus infection in the brain.

References

(1) Peterson KE, Robertson SJ, Portis JL, Chesebro B. Differences in cytokine and chemokine responses during neurological disease induced by polytropic murine retroviruses Map to separate regions of the viral envelope gene. J Virol 2001 Mar;75(6):2848-56.

(2) Peterson KE, Hughes S, Dimcheff DE, Wehrly K, Chesebro B. Separate sequences in a murine retroviral envelope protein mediate neuropathogenesis by complementary mechanisms with differing requirements for tumor necrosis factor alpha. J Virol 2004 Dec;78(23):13104-12.

(3) Clarke M, Newton RW, Klapper PE, Sutcliffe H, Laing I, Wallace G. Childhood encephalopathy: viruses, immune response, and outcome. Dev Med Child Neurol 2006 Apr;48(4):294-300.

(4) Dickson DW, Llena JF, Nelson SJ, Weidenheim KM. Central nervous system pathology in pediatric AIDS. Ann N Y Acad Sci 1993 Oct 29;693:93-106.

(5) Hosoya M, Nunoi H, Aoyama M, Kawasaki Y, Suzuki H. Cytochrome c and tumor necrosis factor-alpha values in serum and cerebrospinal fluid of patients with influenza-associated encephalopathy. Pediatr Infect Dis J 2005 May;24(5):467-70.

(6) Jay V, Becker LE, Blaser S, Hwang P, Hoffman HJ, Humphreys R, et al. Pathology of chronic herpes infection associated with seizure disorder: a report of two cases with tissue detection of herpes simplex virus 1 by the polymerase chain reaction. Pediatr Pathol Lab Med 1995 Jan;15(1):131-46.

(7) Jay V, Hwang P, Hoffman HJ, Becker LE, Zielenska M. Intractable seizure disorder associated with chronic herpes infection. HSV1 detection in tissue by the polymerase chain reaction. Childs Nerv Syst 1998 Jan;14(1-2):15-20.

(8) Kerr JR, Barah F, Chiswick ML, McDonnell GV, Smith J, Chapman MD, et al. Evidence for the role of demyelination, HLA-DR alleles, and cytokines in the pathogenesis of parvovirus B19 meningoencephalitis and its sequelae. J Neurol Neurosurg Psychiatry 2002 Dec;73(6):739-46.

(9) Kimberlin DW. Neonatal herpes simplex infection. Clin Microbiol Rev 2004 Jan;17(1):1-13.

(10) Kirton A, Busche K, Ross C, Wirrell E. Acute necrotizing encephalopathy in caucasian children: two cases and review of the literature. J Child Neurol 2005 Jun;20(6):527-32.

(11) McManus CM, Weidenheim K, Woodman SE, Nunez J, Hesselgesser J, Nath A, et al. Chemokine and chemokine-receptor expression in human glial elements:

induction by the HIV protein, Tat, and chemokine autoregulation. Am J Pathol 2000 Apr;156(4):1441-53.

(12) Mintz M, Rapaport R, Oleske JM, Connor EM, Koenigsberger MR, Denny T, et al. Elevated serum levels of tumor necrosis factor are associated with progressive encephalopathy in children with acquired immunodeficiency syndrome. Am J Dis Child 1989 Jul;143(7):771-4.

(13) Hornig M, Lipkin WI. Infectious and immune factors in the pathogenesis of neurodevelopmental disorders: epidemiology, hypotheses, and animal models. Ment Retard Dev Disabil Res Rev 2001;7(3):200-10.

(14) Kurt-Jones EA, Chan M, Zhou S, Wang J, Reed G, Bronson R, et al. Herpes simplex virus 1 interaction with Toll-like receptor 2 contributes to lethal encephalitis. Proc Natl Acad Sci U S A 2004 Feb 3;101(5):1315-20.

(15) Simard AR, Rivest S. Do pathogen exposure and innate immunity cause brain diseases? Neurol Res 2005 Oct;27(7):717-25.

(16) Yao D, Kuwajima M, Kido H. Pathologic mechanisms of influenza encephalitis with an abnormal expression of inflammatory cytokines and accumulation of mini-plasmin. J Med Invest 2003 Feb;50(1-2):1-8.

(17) Kaisho T, Akira S. Toll-like receptor function and signaling. J Allergy Clin Immunol 2006 May;117(5):979-87.

(18) Diebold SS, Kaisho T, Hemmi H, Akira S, Reis e Sousa. Innate antiviral responses by means of TLR7-mediated recognition of single-stranded RNA. Science 2004 Mar 5;303(5663):1529-31.

(19) Heil F, Hemmi H, Hochrein H, Ampenberger F, Kirschning C, Akira S, et al. Species-specific recognition of single-stranded RNA via toll-like receptor 7 and 8. Science 2004 Mar 5;303(5663):1526-9.

(20) Li H, Zhang J, Kumar A, Zheng M, Atherton SS, Yu FS. Herpes simplex virus 1 infection induces the expression of proinflammatory cytokines, interferons and TLR7 in human corneal epithelial cells. Immunology 2006 Feb;117(2):167-76.

(21) Lund JM, Alexopoulou L, Sato A, Karow M, Adams NC, Gale NW, et al. Recognition of single-stranded RNA viruses by Toll-like receptor 7. Proc Natl Acad Sci U S A 2004 Apr 13;101(15):5598-603.

(22) Schlaepfer E, Audige A, Joller H, Speck RF. TLR7/8 triggering exerts opposing effects in acute versus latent HIV infection. J Immunol 2006 Mar 1;176(5):2888-95.

(23) Mishra BB, Mishra PK, Teale JM. Expression and distribution of Toll-like receptors in the brain during murine neurocysticercosis. J Neuroimmunol 2006 Sep 28.

(24) Becher B, Prat A, Antel JP. Brain-immune connection: immuno-regulatory properties of CNS-resident cells. Glia 2000 Feb 15;29(4):293-304.

(25) Saunders NR, Knott GW, Dziegielewska KM. Barriers in the immature brain. Cell Mol Neurobiol 2000 Feb;20(1):29-40.

(26) Streit WJ, Graeber MB. Heterogeneity of microglial and perivascular cell populations: insights gained from the facial nucleus paradigm. Glia 1993 Jan;7(1):68-74.

(27) Schmidtmayer J, Jacobsen C, Miksch G, Sievers J. Blood monocytes and spleen macrophages differentiate into microglia-like cells on monolayers of astrocytes: membrane currents. Glia 1994 Dec;12(4):259-67.

(28) Ling EA, Wong WC. The origin and nature of ramified and amoeboid microglia: a historical review and current concepts. Glia 1993 Jan;7(1):9-18.

(29) Nakajima K, Kohsaka S. Functional roles of microglia in the brain. Neurosci Res 1993 Aug;17(3):187-203.

(30) Ulvestad E, Williams K, Mork S, Antel J, Nyland H. Phenotypic differences between human monocytes/macrophages and microglial cells studied in situ and in vitro. J Neuropathol Exp Neurol 1994 Sep;53(5):492-501.

(31) Williams K, Ulvestad E, Antel J. Immune regulatory and effector properties of human adult microglia studies in vitro and in situ. Adv Neuroimmunol 1994;4(3):273-81.

(32) Hickey WF, Kimura H. Perivascular microglial cells of the CNS are bone marrow-derived and present antigen in vivo. Science 1988 Jan 15;239(4837):290-2.

(33) Prat A, Biernacki K, Wosik K, Antel JP. Glial cell influence on the human blood-brain barrier. Glia 2001 Nov;36(2):145-55.

(34) Shrikant P, Benveniste EN. The central nervous system as an immunocompetent organ: role of glial cells in antigen presentation. J Immunol 1996 Sep 1;157(5):1819-22.

(35) Tan L, Gordon KB, Mueller JP, Matis LA, Miller SD. Presentation of proteolipid protein epitopes and B7-1-dependent activation of encephalitogenic T cells by IFN-gamma-activated SJL/J astrocytes. J Immunol 1998 May 1;160(9):4271-9.

(36) Magistretti PJ, Pellerin L, Rothman DL, Shulman RG. Energy on demand. Science 1999 Jan 22;283(5401):496-7.

(37) Janzer RC, Raff MC. Astrocytes induce blood-brain barrier properties in endothelial cells. Nature 1987 Jan 15;325(6101):253-7.

(38) Kakinuma Y, Hama H, Sugiyama F, Yagami K, Goto K, Murakami K, et al. Impaired blood-brain barrier function in angiotensinogen-deficient mice. Nat Med 1998 Sep;4(9):1078-80.

(39) Mucke L, Eddleston M. Astrocytes in infectious and immune-mediated diseases of the central nervous system. FASEB J 1993 Oct;7(13):1226-32.

(40) Ridet JL, Malhotra SK, Privat A, Gage FH. Reactive astrocytes: cellular and molecular cues to biological function. Trends Neurosci 1997 Dec;20(12):570-7.

(41) Fearon DT, Locksley RM. The instructive role of innate immunity in the acquired immune response. Science 1996 Apr 5;272(5258):50-3.

(42) Gordon S. Pattern recognition receptors: doubling up for the innate immune response. Cell 2002 Dec 27;111(7):927-30.

(43) Takeda K, Kaisho T, Akira S. Toll-like receptors. Annu Rev Immunol 2003;21:335-76.

(44) Chuang T, Ulevitch RJ. Identification of hTLR10: a novel human Toll-like receptor preferentially expressed in immune cells. Biochim Biophys Acta 2001 Mar 19;1518(1-2):157-61.

(45) Du X, Poltorak A, Wei Y, Beutler B. Three novel mammalian toll-like receptors: gene structure, expression, and evolution. Eur Cytokine Netw 2000 Sep;11(3):362-71.

(46) Medzhitov R, Preston-Hurlburt P, Janeway CA, Jr. A human homologue of the Drosophila Toll protein signals activation of adaptive immunity. Nature 1997 Jul 24;388(6640):394-7.

(47) Takeuchi O, Kawai T, Sanjo H, Copeland NG, Gilbert DJ, Jenkins NA, et al. TLR6: A novel member of an expanding toll-like receptor family. Gene 1999 Apr 29;231(1-2):59-65.

(48) Zhang D, Zhang G, Hayden MS, Greenblatt MB, Bussey C, Flavell RA, et al. A toll-like receptor that prevents infection by uropathogenic bacteria. Science 2004 Mar 5;303(5663):1522-6.

(49) Chuang TH, Ulevitch RJ. Cloning and characterization of a sub-family of human toll-like receptors: hTLR7, hTLR8 and hTLR9. Eur Cytokine Netw 2000 Sep;11(3):372-8.

(50) Rock FL, Hardiman G, Timans JC, Kastelein RA, Bazan JF. A family of human receptors structurally related to Drosophila Toll. Proc Natl Acad Sci U S A 1998 Jan 20;95(2):588-93.

(51) Hornung V, Rothenfusser S, Britsch S, Krug A, Jahrsdorfer B, Giese T, et al. Quantitative expression of toll-like receptor 1-10 mRNA in cellular subsets of human peripheral blood mononuclear cells and sensitivity to CpG oligodeoxynucleotides. J Immunol 2002 May 1;168(9):4531-7.

(52) Zarember KA, Godowski PJ. Tissue expression of human Toll-like receptors and differential regulation of Toll-like receptor mRNAs in leukocytes in response to microbes, their products, and cytokines. J Immunol 2002 Jan 15;168(2):554-61.

(53) Boehme KW, Compton T. Innate sensing of viruses by toll-like receptors. J Virol 2004 Aug;78(15):7867-73.

(54) Takeda K, Akira S. Toll receptors and pathogen resistance. Cell Microbiol 2003 Mar;5(3):143-53.

(55) Akira S. Toll-like receptor signaling. J Biol Chem 2003 Oct 3;278(40):38105-8.

(56) Poltorak A, He X, Smirnova I, Liu MY, Van HC, Du X, et al. Defective LPS signaling in C3H/HeJ and C57BL/10ScCr mice: mutations in Tlr4 gene. Science 1998 Dec 11;282(5396):2085-8.

(57) Qureshi ST, Lariviere L, Leveque G, Clermont S, Moore KJ, Gros P, et al. Endotoxin-tolerant mice have mutations in Toll-like receptor 4 (Tlr4). J Exp Med 1999 Feb 15;189(4):615-25.

(58) Hoshino K, Kaisho T, Iwabe T, Takeuchi O, Akira S. Differential involvement of IFN-beta in Toll-like receptor-stimulated dendritic cell activation. Int Immunol 2002 Oct;14(10):1225-31.

(59) Hayashi F, Smith KD, Ozinsky A, Hawn TR, Yi EC, Goodlett DR, et al. The innate immune response to bacterial flagellin is mediated by Toll-like receptor 5. Nature 2001 Apr 26;410(6832):1099-103.

(60) Medzhitov R. Toll-like receptors and innate immunity. Nat Rev Immunol 2001 Nov;1(2):135-45.

(61) Akira S, Takeda K, Kaisho T. Toll-like receptors: critical proteins linking innate and acquired immunity. Nat Immunol 2001 Aug;2(8):675-80.

(62) Takeuchi O, Hoshino K, Kawai T, Sanjo H, Takada H, Ogawa T, et al. Differential roles of TLR2 and TLR4 in recognition of gram-negative and gram-positive bacterial cell wall components. Immunity 1999 Oct;11(4):443-51.

(63) Takeuchi O, Kaufmann A, Grote K, Kawai T, Hoshino K, Morr M, et al. Cutting edge: preferentially the R-stereoisomer of the mycoplasmal lipopeptide macrophage-activating lipopeptide-2 activates immune cells through a toll-like receptor 2- and MyD88-dependent signaling pathway. J Immunol 2000 Jan 15;164(2):554-7.

(64) Bauer S, Kirschning CJ, Hacker H, Redecke V, Hausmann S, Akira S, et al. Human TLR9 confers responsiveness to bacterial DNA via species-specific CpG motif recognition. Proc Natl Acad Sci U S A 2001 Jul 31;98(16):9237-42.

(65) Hemmi H, Takeuchi O, Kawai T, Kaisho T, Sato S, Sanjo H, et al. A Toll-like receptor recognizes bacterial DNA. Nature 2000 Dec 7;408(6813):740-5.

(66) Hiscott J, Kwon H, Genin P. Hostile takeovers: viral appropriation of the NF-kappaB pathway. J Clin Invest 2001 Jan;107(2):143-51.

(67) MacKichan ML. Toll bridge to immunity. Immune molecules hold promise for vaccine adjuvant discovery. IAVI Rep 2005 Sep;9(4):1-5.

(68) Pasare C, Medzhitov R. Control of B-cell responses by Toll-like receptors. Nature 2005 Nov 17;438(7066):364-8.

(69) Katze MG, He Y, Gale M, Jr. Viruses and interferon: a fight for supremacy. Nat Rev Immunol 2002 Sep;2(9):675-87.

(70) Le BA, Tough DF. Links between innate and adaptive immunity via type I interferon. Curr Opin Immunol 2002 Aug;14(4):432-6.

(71) Pfeffer LM, Dinarello CA, Herberman RB, Williams BR, Borden EC, Bordens R, et al. Biological properties of recombinant alpha-interferons: 40th anniversary of the discovery of interferons. Cancer Res 1998 Jun 15;58(12):2489-99.

(72) Sun S, Zhang X, Tough DF, Sprent J. Type I interferon-mediated stimulation of T cells by CpG DNA. J Exp Med 1998 Dec 21;188(12):2335-42.

(73) Marrack P, Kappler J, Mitchell T. Type I interferons keep activated T cells alive. J Exp Med 1999 Feb 1;189(3):521-30.

(74) Schmid DS, Rouse BT. The role of T cell immunity in control of herpes simplex virus. Curr Top Microbiol Immunol 1992;179:57-74.

(75) Rogge L, D'Ambrosio D, Biffi M, Penna G, Minetti LJ, Presky DH, et al. The role of Stat4 in species-specific regulation of Th cell development by type I IFNs. J Immunol 1998 Dec 15;161(12):6567-74.

(76) Crozat K, Beutler B. TLR7: A new sensor of viral infection. Proc Natl Acad Sci U S A 2004 May 4;101(18):6835-6.

(77) Alexopoulou L, Holt AC, Medzhitov R, Flavell RA. Recognition of double-stranded RNA and activation of NF-kappaB by Toll-like receptor 3. Nature 2001 Oct 18;413(6857):732-8.

(78) Krug A, Luker GD, Barchet W, Leib DA, Akira S, Colonna M. Herpes simplex virus type 1 activates murine natural interferon-producing cells through toll-like receptor 9. Blood 2004 Feb 15;103(4):1433-7.

(79) Lund J, Sato A, Akira S, Medzhitov R, Iwasaki A. Toll-like receptor 9-mediated recognition of Herpes simplex virus-2 by plasmacytoid dendritic cells. J Exp Med 2003 Aug 4;198(3):513-20.

(80) Tabeta K, Georgel P, Janssen E, Du X, Hoebe K, Crozat K, et al. Toll-like receptors 9 and 3 as essential components of innate immune defense against mouse cytomegalovirus infection. Proc Natl Acad Sci U S A 2004 Mar 9;101(10):3516-21.

(81) Du X, Poltorak A, Wei Y, Beutler B. Three novel mammalian toll-like receptors: gene structure, expression, and evolution. Eur Cytokine Netw 2000 Sep;11(3):362-71.

(82) Miller RL, Gerster JF, Owens ML, Slade HB, Tomai MA. Imiquimod applied topically: a novel immune response modifier and new class of drug. Int J Immunopharmacol 1999 Jan;21(1):1-14.

(83) Testerman TL, Gerster JF, Imbertson LM, Reiter MJ, Miller RL, Gibson SJ, et al. Cytokine induction by the immunomodulators imiquimod and S-27609. J Leukoc Biol 1995 Sep;58(3):365-72.

(84) Weeks CE, Gibson SJ. Induction of interferon and other cytokines by imiquimod and its hydroxylated metabolite R-842 in human blood cells in vitro. J Interferon Res 1994 Apr;14(2):81-5.

(85) Harrison CJ, Miller RL, Bernstein DI. Posttherapy suppression of genital herpes simplex virus (HSV) recurrences and enhancement of HSV-specific T-cell memory by imiquimod in guinea pigs. Antimicrob Agents Chemother 1994 Sep;38(9):2059-64.

(86) Chen M, Griffith BP, Lucia HL, Hsiung GD. Efficacy of S26308 against guinea pig cytomegalovirus infection. Antimicrob Agents Chemother 1988 May;32(5):678-83.

(87) Bernstein DI, Harrison CJ, Tomai MA, Miller RL. Daily or weekly therapy with resiquimod (R-848) reduces genital recurrences in herpes simplex virus-infected guinea pigs during and after treatment. J Infect Dis 2001 Mar 15;183(6):844-9.

(88) von KG, Lacey CJ, Gross G, Barrasso R, Schneider A. European course on HPV associated pathology: guidelines for primary care physicians for the

diagnosis and management of anogenital warts. Sex Transm Infect 2000 Jun;76(3):162-8.

(89) Hemmi H, Kaisho T, Takeuchi O, Sato S, Sanjo H, Hoshino K, et al. Small anti-viral compounds activate immune cells via the TLR7 MyD88-dependent signaling pathway. Nat Immunol 2002 Feb;3(2):196-200.

(90) Jurk M, Heil F, Vollmer J, Schetter C, Krieg AM, Wagner H, et al. Human TLR7 or TLR8 independently confer responsiveness to the antiviral compound R-848. Nat Immunol 2002 Jun;3(6):499.

(91) Lee J, Chuang TH, Redecke V, She L, Pitha PM, Carson DA, et al. Molecular basis for the immunostimulatory activity of guanine nucleoside analogs: activation of Toll-like receptor 7. Proc Natl Acad Sci U S A 2003 May 27;100(11):6646-51.

(92) Heil F, hmad-Nejad P, Hemmi H, Hochrein H, Ampenberger F, Gellert T, et al. The Toll-like receptor 7 (TLR7)-specific stimulus loxoribine uncovers a strong relationship within the TLR7, 8 and 9 subfamily. Eur J Immunol 2003 Nov;33(11):2987-97.

(93) Gorden KK, Qiu X, Battiste JJ, Wightman PP, Vasilakos JP, Alkan SS. Oligodeoxynucleotides differentially modulate activation of TLR7 and TLR8 by imidazoquinolines. J Immunol 2006 Dec 1;177(11):8164-70.

(94) Gorden KK, Qiu XX, Binsfeld CC, Vasilakos JP, Alkan SS. Cutting edge: activation of murine TLR8 by a combination of imidazoquinoline immune response modifiers and polyT oligodeoxynucleotides. J Immunol 2006 Nov 15;177(10):6584-7.

(95) Jurk M, Kritzler A, Schulte B, Tluk S, Schetter C, Krieg AM, et al. Modulating responsiveness of human TLR7 and 8 to small molecule ligands with T-rich phosphorothiate oligodeoxynucleotides. Eur J Immunol 2006 Jul;36(7):1815-26.

(96) Kadowaki N, Ho S, Antonenko S, Malefyt RW, Kastelein RA, Bazan F, et al. Subsets of human dendritic cell precursors express different toll-like receptors and respond to different microbial antigens. J Exp Med 2001 Sep 17;194(6):863-9.

(97) Bourke E, Bosisio D, Golay J, Polentarutti N, Mantovani A. The toll-like receptor repertoire of human B lymphocytes: inducible and selective expression of TLR9 and TLR10 in normal and transformed cells. Blood 2003 Aug 1;102(3):956-63.

(98) Bernasconi NL, Onai N, Lanzavecchia A. A role for Toll-like receptors in acquired immunity: up-regulation of TLR9 by BCR triggering in naive B cells and constitutive expression in memory B cells. Blood 2003 Jun 1;101(11):4500-4.

(99) Fonteneau JF, Larsson M, Beignon AS, McKenna K, Dasilva I, Amara A, et al. Human immunodeficiency virus type 1 activates plasmacytoid dendritic cells and concomitantly induces the bystander maturation of myeloid dendritic cells. J Virol 2004 May;78(10):5223-32.

(100) Siegal FP, Kadowaki N, Shodell M, Fitzgerald-Bocarsly PA, Shah K, Ho S, et al. The nature of the principal type 1 interferon-producing cells in human blood. Science 1999 Jun 11;284(5421):1835-7.

(101) Rissoan MC, Soumelis V, Kadowaki N, Grouard G, Briere F, de Waal MR, et al. Reciprocal control of T helper cell and dendritic cell differentiation. Science 1999 Feb 19;283(5405):1183-6.

(102) Cella M, Jarrossay D, Facchetti F, Alebardi O, Nakajima H, Lanzavecchia A, et al. Plasmacytoid monocytes migrate to inflamed lymph nodes and produce large amounts of type I interferon. Nat Med 1999 Aug;5(8):919-23.

(103) Glass JD, Fedor H, Wesselingh SL, McArthur JC. Immunocytochemical quantitation of human immunodeficiency virus in the brain: correlations with dementia. Ann Neurol 1995 Nov;38(5):755-62.

(104) Glass JD, Wesselingh SL, Selnes OA, McArthur JC. Clinical-neuropathologic correlation in HIV-associated dementia. Neurology 1993 Nov;43(11):2230-7.

(105) Kolson DL, Lavi E, Gonzalez-Scarano F. The effects of human immunodeficiency virus in the central nervous system. Adv Virus Res 1998;50:1-47.

(106) Lackner AA, Dandekar S, Gardner MB. Neurobiology of simian and feline immunodeficiency virus infections. Brain Pathol 1991 Apr;1(3):201-12.

(107) Portis JL, Czub S, Robertson S, McAtee F, Chesebro B. Characterization of a neurologic disease induced by a polytropic murine retrovirus: evidence for differential targeting of ecotropic and polytropic viruses in the brain. J Virol 1995 Dec;69(12):8070-5.

(108) Robertson SJ, Hasenkrug KJ, Chesebro B, Portis JL. Neurologic disease induced by polytropic murine retroviruses: neurovirulence determined by efficiency of spread to microglial cells. J Virol 1997 Jul;71(7):5287-94.

(109) Hasenkrug KJ, Robertson SJ, Porti J, McAtee F, Nishio J, Chesebro B. Two separate envelope regions influence induction of brain disease by a polytropic murine retrovirus (FMCF98). J Virol 1996 Jul;70(7):4825-8.

(110) Robertson MN, Miyazawa M, Mori S, Caughey B, Evans LH, Hayes SF, et al. Production of monoclonal antibodies reactive with a denatured form of the Friend murine leukemia virus gp70 envelope protein: use in a focal infectivity

assay, immunohistochemical studies, electron microscopy and western blotting. J Virol Methods 1991 Oct;34(3):255-71.

(111) Rozen S, Skaletsky HJ. Primer3 on the WWW for general users and for biologist programmers. Bioinformatics Methods and Protocols: Methods in Molecular Biology 2000;365-86.

(112) Peterson KE, Errett JS, Wei T, Dimcheff DE, Ransohoff R, Kuziel WA, et al. MCP-1 and CCR2 contribute to non-lymphocyte-mediated brain disease induced by Fr98 polytropic retrovirus infection in mice: role for astrocytes in retroviral neuropathogenesis. J Virol 2004 Jun;78(12):6449-58.

(113) Peterson KE, Evans LH, Wehrly K, Chesebro B. Increased proinflammatory cytokine and chemokine responses and microglial infection following inoculation with neural stem cells infected with polytropic murine retroviruses. Virology 2006 Jul 26.

(114) Lee Y, Su M, Messing A, Brenner M. Astrocyte heterogeneity revealed by expression of a GFAP-LacZ transgene. Glia 2006 May;53(7):677-87.

(115) Zhang L, Zhao W, Li B, Alkon DL, Barker JL, Chang YH, et al. TNF-alpha induced over-expression of GFAP is associated with MAPKs. Neuroreport 2000 Feb 7;11(2):409-12.

(116) Williams AE, Lawson LJ, Perry VH, Fraser H. Characterization of the microglial response in murine scrapie. Neuropathol Appl Neurobiol 1994 Feb;20(1):47-55.

(117) Kadowaki N, Liu YJ. Natural type I interferon-producing cells as a link between innate and adaptive immunity. Hum Immunol 2002 Dec;63(12):1126-32.

(118) Burzyn D, Rassa JC, Kim D, Nepomnaschy I, Ross SR, Piazzon I. Toll-like receptor 4-dependent activation of dendritic cells by a retrovirus. J Virol 2004 Jan;78(2):576-84.

(119) Haynes LM, Moore DD, Kurt-Jones EA, Finberg RW, Anderson LJ, Tripp RA. Involvement of toll-like receptor 4 in innate immunity to respiratory syncytial virus. J Virol 2001 Nov;75(22):10730-7.

(120) Kurt-Jones EA, Popova L, Kwinn L, Haynes LM, Jones LP, Tripp RA, et al. Pattern recognition receptors TLR4 and CD14 mediate response to respiratory syncytial virus. Nat Immunol 2000 Nov;1(5):398-401.

(121) Mandelberg A, Tal G, Naugolny L, Cesar K, Oron A, Houri S, et al. Lipopolysaccharide hyporesponsiveness as a risk factor for intensive care unit hospitalization in infants with respiratory syncitial virus bronchiolitis. Clin Exp Immunol 2006 Apr;144(1):48-52.

(122) Tal G, Mandelberg A, Dalal I, Cesar K, Somekh E, Tal A, et al. Association between common Toll-like receptor 4 mutations and severe respiratory syncytial virus disease. J Infect Dis 2004 Jun 1;189(11):2057-63.

(123) Wang T, Town T, Alexopoulou L, Anderson JF, Fikrig E, Flavell RA. Toll-like receptor 3 mediates West Nile virus entry into the brain causing lethal encephalitis. Nat Med 2004 Dec;10(12):1366-73.

(124) Wang J, Shao Y, Bennett TA, Shankar RA, Wightman PD, Reddy LG. The functional effects of physical interactions among Toll-like receptors 7, 8, and 9. J Biol Chem 2006 Dec 8;281(49):37427-34.

(125) Jurk M, Heil F, Vollmer J, Schetter C, Krieg AM, Wagner H, et al. Human TLR7 or TLR8 independently confer responsiveness to the antiviral compound R-848. Nat Immunol 2002 Jun;3(6):499.

(126) Crozat K, Beutler B. TLR7: A new sensor of viral infection. Proc Natl Acad Sci U S A 2004 May 4;101(18):6835-6.

(127) Ma Y, Li J, Chiu I, Wang Y, Sloane JA, Lu J, et al. Toll-like receptor 8 functions as a negative regulator of neurite outgrowth and inducer of neuronal apoptosis. J Cell Biol 2006 Oct 23;175(2):209-15.

(128) Beignon AS, McKenna K, Skoberne M, Manches O, DaSilva I, Kavanagh DG, et al. Endocytosis of HIV-1 activates plasmacytoid dendritic cells via Toll-like receptor-viral RNA interactions. J Clin Invest 2005 Nov;115(11):3265-75.

(129) Lee HK, Lund JM, Ramanathan B, Mizushima N, Iwasaki A. Autophagy-Dependent Viral Recognition by Plasmacytoid Dendritic Cell. Science 2007 Feb 1.

(130) Nussbaum O, Roop A, Anderson WF. Sequences determining the pH dependence of viral entry are distinct from the host range-determining region of the murine ecotropic and amphotropic retrovirus envelope proteins. J Virol 1993 Dec;67(12):7402-5.

(131) Corbin ME, Pourciau S, Morgan TW, Boudreaux M, Peterson KE. Ligand up-regulation does not correlate with a role for CCR1 in pathogenesis in a mouse model of non-lymphocyte mediated neurological disease. J Neurovirol 2006;12:1-10.

(132) Krug A, Towarowski A, Britsch S, Rothenfusser S, Hornung V, Bals R, et al. Toll-like receptor expression reveals CpG DNA as a unique microbial stimulus for plasmacytoid dendritic cells which synergizes with CD40 ligand to induce high amounts of IL-12. Eur J Immunol 2001 Oct;31(10):3026-37.

(133) Gorden KB, Gorski KS, Gibson SJ, Kedl RM, Kieper WC, Qiu X, et al. Synthetic TLR agonists reveal functional differences between human TLR7 and TLR8. J Immunol 2005 Feb 1;174(3):1259-68.

(134) Ito T, Amakawa R, Kaisho T, Hemmi H, Tajima K, Uehira K, et al. Interferon-alpha and interleukin-12 are induced differentially by Toll-like receptor 7 ligands in human blood dendritic cell subsets. J Exp Med 2002 Jun 3;195(11):1507-12.

Vita

Stephanie Lewis was born the youngest of three children in Port Jefferson, New York, to Frank and Judy Lewis. At age three, she moved to Texas and later moved to St. Louis, Missouri, at age eleven. In high school she volunteered at the Wolf Sanctuary and moved to Minnesota to pursue a degree in fisheries and wildlife, only to change her major to pre-vet. She went on to attend veterinary school and obtain her Doctor of Veterinary Medicine from the University of Missouri-College of Veterinary Medicine. After working a year in private practice, she moved to Baton Rouge, Louisiana, to pursue a residency in laboratory animal medicine. She hopes to continue her involvement in research by pursuing a career as a clinical laboratory animal veterinarian.